

We are IntechOpen, the world's leading publisher of Open Access books Built by scientists, for scientists

6,900

Open access books available

186,000

International authors and editors

200M

Downloads

Our authors are among the

154

Countries delivered to

TOP 1%

most cited scientists

12.2%

Contributors from top 500 universities



WEB OF SCIENCE™

Selection of our books indexed in the Book Citation Index
in Web of Science™ Core Collection (BKCI)

Interested in publishing with us?
Contact book.department@intechopen.com

Numbers displayed above are based on latest data collected.
For more information visit www.intechopen.com



Metal Nanoparticles as Emerging Green Catalysts

Ahmad Alshammari, V. Narayana Kalevaru and
Andreas Martin

Additional information is available at the end of the chapter

<http://dx.doi.org/10.5772/63314>

Abstract

Green nanotechnology is defined as the technology applied for building clean technology by which one can reduce the potential risks of environment and also improve human health conditions. It is linked with the implementation of products of nanotechnology and its process of manufacturing. Green nanotechnology synthesizes new nanoproducts with improved properties in such a way that they can substitute some of the existing low-quality products. The main motive of developing new nanoproducts is to enhance sustainability and also to make them more environment friendly. In particular, nanoscale materials (e.g., nanoparticles) can be defined as those having characteristic length scale lying within the nanometric range, that is, in the range between one and several hundreds of nanometers. Within this length scale, the properties of matter are sufficiently different from individual atoms/molecules or from bulk materials. The primary objective of this chapter is to provide comprehensive overview about metal nanoparticles (MNPs) and its application as emerging green catalysts. This chapter contains six sections in total. Section 1 starts with a general introduction, recent progress, and brief summary of the application of MNPs as green catalyst. Section 2 reviews the preparation and characterization of supported metal nanoparticles for a wide range of catalytic applications. Section 3 presents the catalytic properties of supported metal nanoparticles. Section 4 describes briefly some of the most commonly reported supported MNPs in different green catalytic applications. Section 5 concentrates on our own results that related to the application of supported MNPs in catalysis. In this section, the oxidation of benzyl alcohol to benzaldehyde, the production of adipic acid from cyclohexane, the photodegradation of dyes using green route will be discussed. Finally, Section 6 describes the summary of main points and also presents an outlook of the application of MNPs in green chemistry.

Keywords: metal nanoparticles (MNPs), MNPs for environmental application, green catalyst, photocatalysis, MNPs characterization, oxidation reaction

1. Introduction to metal nanoparticles

Materials whose length lies within the nanometric range of one to several hundred nanometers are known as nanoscale materials or nanoparticles [1]. Matter at this scale is characterized by significantly different material properties than molecules, atoms, or bulk items [2]. Because of this, the field of *Nanoscience* was coined to address this relatively novel scientific field. Although the concept of this scientific area is not new, contemporary science is constantly discovering new and favorable applications for both the manufacture sector and academia, which has cast *Nanoscience* as a burgeoning and exciting field. The applications referred to are diverse, and range from environmental development to consumer products, and even therapeutic use (**Figure 1**).

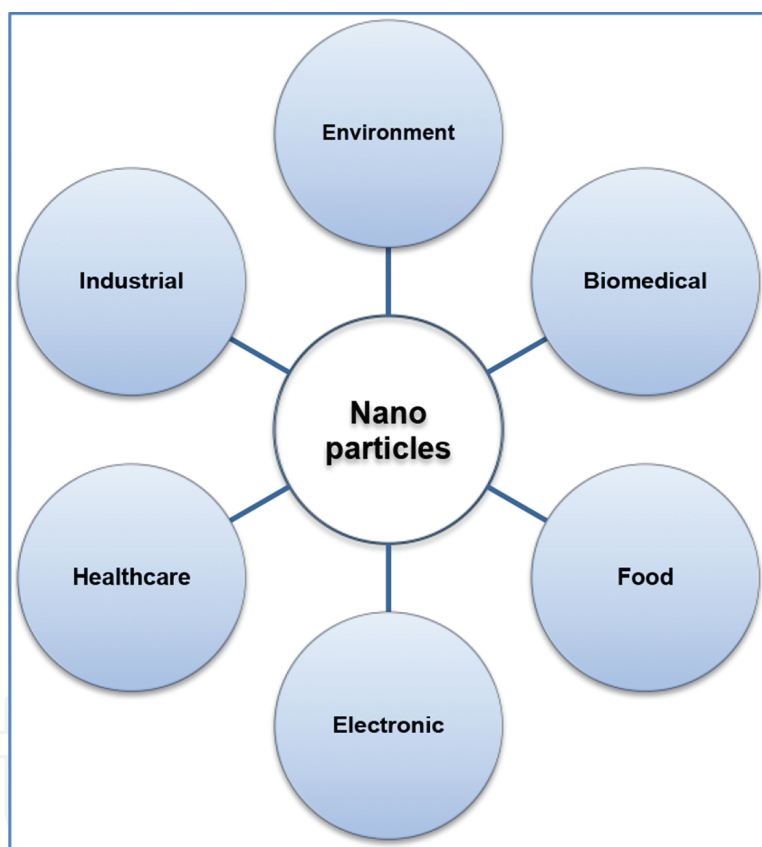


Figure 1. Potential application of nanoparticles in various fields.

Nanoparticles can take many forms, including powder, crystal, and cluster formulae. Nanopowder is used to describe mixtures of fine powder, whereas ultrafine particle mixtures are described as nanocrystals [2]. Clusters can be further classified as nanoclusters if they have a narrow size distribution in the range of 1–10 nm and a minimum of one dimension. Prior to the 1700s, nanoparticle use was limited to high-quality glass, pottery, and tile production. In the mid-nineteenth century, Michael Faraday began to explore nanoparticle stability. At the beginning of the twentieth century, Mie conducted research into nanoparticle color properties.

Shortly thereafter, Richard Zsigmondy received the 1925 Nobel Prize in Chemistry for his work on colloidal suspension of gold nanoparticles using ultramicroscopic techniques.

Metal nanoparticles (MNPs) are deemed to be likely candidates for catalysis due to their relatively large surface area per volume or weight unit as compared with bulk metal, meaning heterogeneous MNPs catalysts typically function on metal surfaces [3]. A variety of techniques are used to develop supports for industrial metal catalysts, which are frequently inorganic and characterized by highly dispersed metals and voluminous surface area. Metal particles tend to be ensemble affairs, consisting of more than one particle in a range of forms and dimensions. Polyhedral particles are formed from the interaction of MNPs with the inorganic supports. Silica gel, activated charcoal, and alumina, among others, are examples of transition metals that are formed from metal particles distributed onto inorganic supports. These are superior to metal powders for numerous reasons, including their stable thermic capacity, diminished cost, greater surface area, and efficacious use of MNPs in the form of wide dispersion.

The electrochemical makeup of particularly dimensioned MNPs allows them to be used as catalysts. As compared with bulk metallic catalysts, greater surface area and measured edge step ratio result in higher outputs. MNPs also are well suited to stereoselective synthesis. MNPs have been increasingly examined in recent years due to their catalytic properties in a range of contexts, for example, as a surfactant for water-soluble polymer, resins, vesicles, and so on. Other examples are the reactions including Fischer-Tropsch, isomerization, and hydroformylation, etc., which also use nanoparticles such as Rh, Pt, Ir, Au, and Pd as catalysts [4]. The size of the metal particles holds great influence over the catalytic abilities of the metal. Additionally, if one looks to the use of gold nanoparticles in catalysis, the size of the gold particle is directly linked to catalytic activity and/or selectivity. Gold particles with diameters less than 10 nm are deemed to be very active catalysts, while such activity considerably diminishes as the Au diameter increases, and also virtually disappears when the diameter is measured in micrometers range [5, 6].

MNPs are functionalized in many situations as they typically have greater stability in solutions as compared to nonfunctionalized metallic nanoparticles. This is because the nonfunctionalized particles present with a reduced surface area and thus lower catalytic ability due to their tendency to aggregate while in solution. Although ligands can be used to avoid aggregation, they have the consequence of altering catalyst functionality. Nanocatalysts can also be functionalized using polymers and oligomers. Typically, catalytic nanoparticles have been implemented in tandem with polymer matrices; otherwise, they were detained on solid supports [7]. The petrochemical industry has a long history of utilizing supported metal catalysts, particularly Pt, which is used for naphtha reforming. However, new techniques that employ electrostatic interaction forces are now being created that will enable stable catalytic aggregate of a preferred form [8]. Multilayer polyelectrolyte film is formed through the adsorption of metal ions (Ag^+ , Pt^{2+}) [9].

MNPs are primarily defined by their size; so, it follows that size is the real driving force of their catalytic capabilities. Because metal particle surface area is inversely proportional to squared nanoparticle diameter, as particles decrease in size, the surface area increases. This decreasing size results in greater catalytic activity, as all chemical reactions occur on the

catalyst surface [10, 11]. The rate of reaction is also influenced by particle size in case of some chemical reactions. In these instances, slower reactions are caused by reduced nanocatalyst size. For example, when using Pt nanocatalysts for the generation of photochemical hydrogen, it is ideal to use catalysts with 3 nm particle diameters. Any other size, greater or less, will slow down the chemical reaction [12]. Catalyst selectivity is also affected by size. For example, when creating monoene in cyclopentadiene partial hydrogenation, a size of <2 nm is considered ideal. However, the particles having larger size will alter the reaction's selectivity due to the Pt nanoparticles' steric effects [13].

In addition, material arrangement of nanocatalysts also plays a key role in catalytic activity, wherein the addition of other metals can result in added value. The ligand and ensemble effects are most often cited as the cause of this effect. Because of the redox potential of metals, the reaction is also impacted by nanocatalysts' core-shell construction [14]. As an example, the ratio of Pd/Pt = 4 is considered to be the ideal nanoparticle ratio for high performance during the process of selective partial hydrogenation of 1,3-cyclooctadiene to cyclooctene. However, these bimetallic nanoparticles will experience diminished catalytic activity if such ratio is altered. The ligands effect resulting from the incidence of Pt at the particle cores means the bimetallic catalysts have greater activity levels as compared with monometallic Pd catalysts [15].

The catalytic performances of supported MNPs are dependent on catalyst stability, which can be proven when considering the relationship between MNP size and catalytic activity. However, agglomeration means naked colloidal nanoparticles, which are already thermodynamically unstable, are further unstable in the long run. In order to prevent such agglomeration, these particles must be stabilized for the long term, which can be achieved in a number of ways. Two methods would be supporting them on a solid surface or coordination with ligands/anionic species [16]. Metallic nanocatalysts can be stabilized in either aqueous or nonaqueous solutions using polymers, as is the case with the use of polystyrene-*b*-poly-4-vinylpyridine being used to ensure Pd is stable during a Heck reaction in which a styrene and 4-bromoacetophenone coupling takes place [17].

2. Synthesis and characterization of metal nanoparticles

2.1. Synthesis methods [1, 2]

Metal particle synthesis typically takes place in one of two ways: top-down or bottom-up, as shown in **Figure 2**. The top-down approach uses an external force to pressure bulk materials, eventually causing these materials to break down into smaller components by means of mechanical, chemical, or some other energy sources. A bottom-up approach takes place in a reverse tactic, growing precursor particle size by using chemical reactions to combine atomic or molecular species. It should be noted that the top-down approach is considered to be a physical method while the bottom-up approach is chemical, although both approaches can be applied in a range of states, including liquid, solid, gas, supercritical fluids, or vacuum. The final desired outcome and manufacturer must play into the choice between the two methods.

Because size and shape of the metal particles is the most vital aspect to be altered for improved application performance, it is a vital aspect to take into account for catalysis as an example. This section will address some selected methods for fabricating metal nanoparticles, including physical and chemical methods.

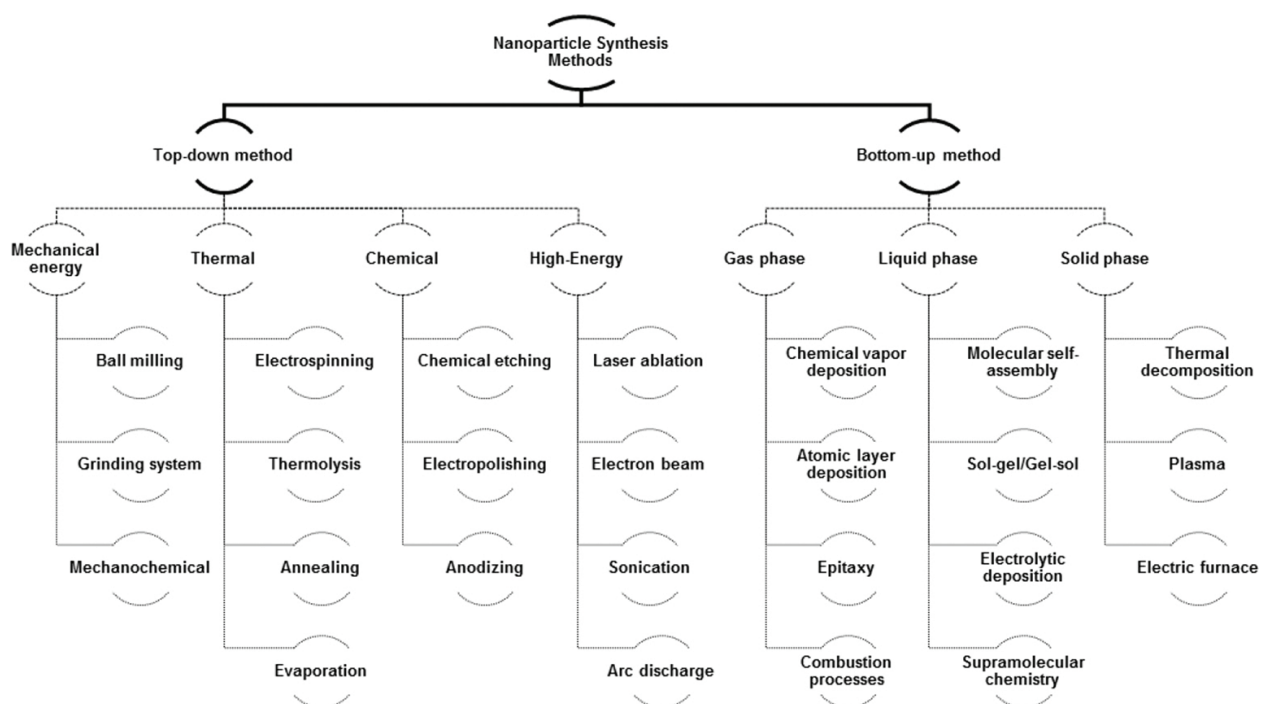


Figure 2. Main synthetic approaches for fabricating metal nanoparticles.

2.1.1. Chemical methods

When it comes to synthesizing metal nanoparticles from a range of source materials, chemical methods have become a reliable technique. They are relatively simple and are implemented under mild conditions. The following section will examine the production process for isolated nanocrystals dispersible in solvents (sols).

2.1.1.1. Chemical reduction

The most ancient and widely used chemical method for synthesis of nanoparticles is the reduction of metallic ions in solution. In ion reduction method, metal ions are reduced by providing some extra energy and using the different types of chemical reductants. The provided energy is used to decompose the material, and usually, photo energy, electricity, or thermal energy is used. It is the most frequent chemical method used for the production of stable metallic nanoparticles. Turkevich used this method to produce spherical nanoparticles of gold by reducing the gold hydrochlorate solution with sodium tricitrate [18]. Nanoparticles of gold can also be produced by reducing the solution of chloroauric acid; this reaction reduces Au^{+3} ions to Au^+ and further into Au^0 . Brust method and Perrault method were also used to

produce metallic nanoparticles; the main theme of both these methods is the same as in Turkevich method with different reducing and anticoagulant agents.

2.1.1.2. Coreduction of mixed ions

Coreduction of mixed ions is similar to chemical reduction in many ways. However, this method is mainly used for preparing bimetallic nanoparticles. The preparation of the colloidal dispersions of bimetallic nanoparticles containing gold can be prepared using chemical methods [2]. Coreduction is the simplest preparative method of bimetallic nanoparticles. In this method, metal ions of two or more metals are usually reduced by suitable reductants (e.g., citrate) [18]. The average diameter of bimetallic nanoparticles depends on the metal composition.

2.1.2. Physical methods

Physical methods require solid material to be evaporated into supersaturated vapor, which supports the homogenous nucleation of nanoparticles in order to prepare MNPs [1]. This also allows particle size to be temporarily controlled either by introducing gas molecules that collide with the particles, or by momentarily halting the evaporation source. Because growth occurs over a matter of milliseconds or seconds, experimental parameters must be securely controlled. Recent years have seen the development of several particular methods that can be categorized according to their use of solid or liquid (vapor) precursors, as well as the energy source employed.

2.1.3. Other methods

In this section, some additional methods for preparing nanoparticles are reviewed. These methods include both chemical and physical methods.

2.1.3.1. Vapor synthesis

In order to create conditions that support particle nucleation, a hot wall reactor is used on material, and other variable factors (pressure and temperature) are adjusted during the vapor phase. The vapor synthesis model is favored for multicomponent or bimetallic nanoparticles. This process has been recently used by Schmechel to translate organometallic yttrium and europium to europium-doped yttria nanoparticles [19].

2.1.3.2. Sputtering

Inert gas in the form of high-velocity ion is applied in this technique to vaporize material from a solid surface. The application results in the solid surface ejecting atoms, and is typically done in a vacuum state. It is also possible to deploy electrons in the place of atoms [20]. This technique is preferred for its ability to create nanoparticles with a composition matching that of the targeted material [21].

2.1.3.3. Laser reactors

This technique uses laser beams to heat a substrate in the presence of an inert gas. Laser beam energy is absorbed by the substrate during the vapor phase, resulting in direct warming. As a result, temperature increases due to collision, and despite the fact that inert or carrier are not directly heated. The dropping temperature of inert gas causes supersaturation and prompts the formation of nanoparticles on the reactor wall [22]. Laser pyrolysis is typically carried out with ruby laser and CO₂-type lasers. The fact that there is no need to use a heat wall is a major benefit of this method. This avoids contamination, which can otherwise be introduced by the heat wall, making this method more efficient than sputtering methods. However, the technique has drawbacks as well—the use of laser increases costs [23].

2.1.3.4. Flame reactors

Nanoparticles can also be produced using flame, whose heat initiates a reaction resulting in condensable monomers that are frequently in agglomerate form. The flame reactor method is considered cost-effective [24]. For instance, TiCl₄ can be heated and oxidized in the presence of flame, resulting in the nanoparticles of TiO₂. This is just one example on the use of this method. Small modifications allow flame reactors to be used for complex and free agglomerate outputs as well [25].

2.1.3.5. Plasma reactors

Nanoparticle production can be initiated using plasma as an energy source. This is because plasma temperature is high enough to isolate atoms and radicals from the substrate, which results in nanoparticles establishing themselves on the cooling gases. Dc arc plasma, dc plasma jet, and radio-frequency (rf) induction plasma are the most frequently used plasmas in this method, which can be used to generate multicomponent nanoparticles [26, 27]. It is possible to speed up production by introducing cold gas to plasma-formed vapors, but this can cause destruction of nanoparticle homogeneity [27].

2.1.3.6. Wire electrical explosion

Heat and vapors are produced in this method by passing a high current through a metallic wire. It is useful when dealing with metals that are difficult to vaporize in a furnace due to their high boiling point (Si, C) [28]. The method has previously been used to create 2–4 nm Si nanoparticles using Ar inert gas as a carrier. Reaction and carrier duties are carried out by reactive gases to form binary metallic and multicomponent nanoparticles [29].

2.1.3.7. Expansion–cooling

Abrupt expansion and cooling are used to stimulate homogenous nucleation by passing condensed gas through a nozzle, resulting in gas expansion and temperature reduction. Particle size is then able to be altered using pressure change: bigger sizes are achieved using higher pressure. For example, N₂ gas in a subsonic nozzle will result in 100 nm particles if 2

bar pressure is applied. However, using 0.75 bar pressure under the same conditions produces 5 nm particles [20].

2.1.3.8. Electrospray systems

This is the simplest means of creating nanoparticles and requires a small droplet of dilute solution to be evaporated. The intended matter is made into diluted solution and dried in small droplets of 1 μm , producing nanoparticles. However, it is difficult to create this very small size of droplet required, and hence there is an added challenge that the solvent can introduce some impurities [30].

2.2. Characterization methods

Nanoscale materials have a unique set of properties, making them suitable for a variety of applications and resulting in them being a focal point for a range of researches. Deep understanding of the properties of metal particles at nanoscale level is necessary to understand the nature of active sites, which in turn can help to find and tune the key performance signs. Several techniques exist that are designed to characterize nanoparticles, although none of these are able to supply full information regarding investigated materials. For this reason, several techniques must be used to categorize each sample in order to understand the size, structure, and catalytic properties. **Figure 3** depicts various methods of analyses for MNPs.

Characterization Method	• Information obtained
Dynamic light scattering (DLS)	• Size and size distribution of MNPs in solution
UV-Vis spectrum	• Formation of colloidal MNPs (Plasmon band)
X-ray diffraction (XRD)	• Crystal structure and size, chemical composition
Nuclear magnetic resonance (NMR)	• Molecular physics, crystals and non-crystalline materials
X-ray photoelectron spectroscopy (XPS)	• Surface composition of supported MNPs
Transmission electron microscopy (TEM) Scanning electron microscopy (SEM)	• Size and Morphology of MNPs
Energy Dispersive X-Ray (EDX)	• Element and distribution of MNPs
Scanning tunneling microscope	• Size and structure of MNPs

Figure 3. Summary of some selected characterization techniques of MNPs.

Common means of characterizing MNPs include transmission electron microscopy (TEM) and scanning electron microscopy (SEM). Other common techniques include X-ray photoelectron spectroscopy (XPS), UV spectroscopy, atomic force microscopy, powder X-ray diffractometry (XRD), and dynamic light scattering (DLS). UV spectroscopy and Fourier transformed infrared spectroscopy (FTIR) methods would be combined to examine gold and palladium nanoparti-

cles, as described elsewhere [31, 32]. Conversely, silver nanoparticles would be examined using TEM, high-resolution TEM, and selected area diffraction pattern (SAED) [33]. Finally, X-ray diffraction, SEM, and FTIR would be combined to examine magnetite, Ag, zinc, and Au nanoparticles [33–35].

3. Catalytic properties of supported metal nanoparticles

Supported metal nanoparticles (SMNPs) are used today in several application fields such as sensors, nanoelectronics, medical-technical applications, and in heterogeneous catalysis [36, 37]. In general, SMNPs consist of metal nanoparticles (MNPs) from transition metal or noble metal pools that are deposited on high surface area supports (150–1200 m²/g). In general, the metal load of supported metal catalysts is generally in the range of 0.5 up to 10 wt.% (even higher in rare cases). MNPs are often in a size range of roughly 1–30 nm. Such particles reveal chemical and physical properties that are intermediate between those of a single metal atom and a bulky metal particle of a size much larger than 100 nm. However, careful handling is important, that is, once activated, most of these SMNP solids are pyrophoric by contact with oxygen.

The activity of supported metal catalysts in heterogeneously catalyzed reactions is mainly determined by the shape and size of the metal species (i.e., MNPs) deposited onto the support, because only surface metal atoms might take part in a chemical reaction [37–39]. Heterogeneous catalyst performance is very sensitive to particle size, because the structure of the solid surface and the electronic properties may significantly change depending on the size of the MNPs [37, 38]. For example, the activation energy for CO dissociation and the heat of adsorption for CO alter with changing size of MNPs. These changing properties affect its performance in several CO-converting reactions like Fischer-Tropsch (FT) synthesis for the manufacture of hydrocarbons from gas synthesis. Supported Au-containing catalysts show similar size effects with respect to applied supports [40, 41]. Au nanoparticles on alumina smaller than 4 nm show complete conversion in ethylene glycol oxidation, but increasing nanoparticle diameter above 5 nm leads to significant drop to roughly 40% conversion only [40].

Therefore, one crucial property of supported heterogeneous MNP catalysts is that they contain the metals as finely dispersed particles on the support surface, in general [38, 42, 43]. Incidentally, the term dispersion describes the degree of metal distribution (**Figure 4**); a dispersion degree of close to 1 means that all offered metal atoms exist in an atomic dispersed monolayer at the surface, whereas a dispersion degree of almost 0 says that only one large particle is present [44, 45]. Thus, the dispersion degree is inversely proportional to the MNP size. The dispersion degree might be determined by chemical methods such as hydrogen or CO chemisorption; a nice overview on CO chemisorption on metal particles is given by Hammer et al. [46]. However, one has to know adsorption chemistry well to draw the right conclusions from experimental data; for example, CO can be adsorbed on Pt surfaces linearly, bridged or multibound, as proven by different bands obtained from FTIR spectra [47]. Thus, the number of CO atoms adsorbed on a nanoparticle surface does not necessarily mirror the number of

surface atoms and the dispersion degree. Nowadays, DFT calculations and several adsorption models help to refine experimental data [48]. Small-angle X-ray scattering (SAXS), X-ray diffraction, and TEM can also be applied; in addition, several in situ studies can be included for characterizations [37, 49]. The latter needs some more intense sample preparation and examination efforts to get statistically reliable conclusions.

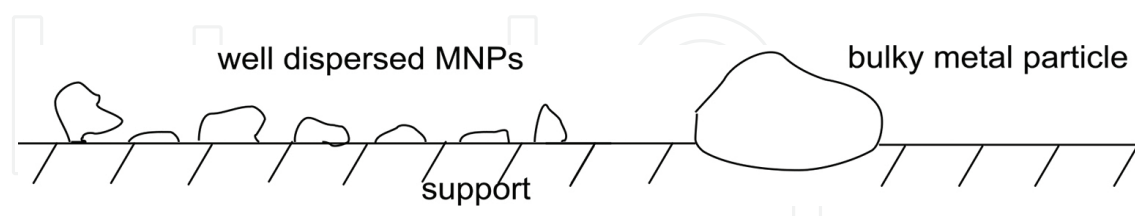


Figure 4. Well-dispersed metal nanoparticles (MNPs) versus a large metal particle on a support surface.

Besides MNPs' size and shape, the catalytic properties of such particles might be influenced by a second metal, the so-called bimetallic catalysts. The addition of a second metal often leads to alloys showing quite different electronic and also structural properties. Some examples are the formation of PtNi or Pt-bimetal SMNPs for electrocatalytic applications [50, 51] or AuNi SMNPs for steam reforming of hydrocarbons [52]. Moreover, support properties strongly influence the catalytic performance of SMNPs. Matsumura and Nakamori describe in detail the effect of various supports on catalytic properties of such nickel catalysts in the steam reforming of methane (SRM) reaction [53]. Au nanoparticles (<4 nm) on alumina reveal full conversion in glycol conversion, whereas Au nanoparticles on carbon need a size of 7–8 nm to reach complete conversion [40]. Support-metal interaction is studied in detail for several catalyst systems and also reviewed in Ref. [54].

Mainly hydrogenation (dehydrogenation), oxidation, automotive off-gas cleaning, and C-C coupling reactions run on such SMNP catalysts [42, 43, 55]. Most of these reactions proceed in the gas phase, and various examples of liquid phase or trickle bed reactions are also known. In particular, in the latter cases, loss of active MNPs by leaching might be a catalyst deactivation reason. Further deactivation reasons are due to MNPs sintering by high reaction temperatures or easy movability on a support surface. Furthermore, MNPs might deactivate by accumulation of products or oligomers and coke-like products on their surface. In general, the latter can be easily regenerated by hydrogen or air (oxygen) treatment in case of oxidic carriers with subsequent reduction. Au, Pd, Rh, Ru, Ni, or Ag are the mostly widely used MNPs for the above-mentioned transformations [55]. In general, various oxidic supports, such as diverse aluminas, silicas, titanias, etc., and several carbon materials, are usually used as supports for the MNPs. White et al. recently summarized various synthesis protocols in a concise review [55]. Impregnation, coprecipitation, and deposition-precipitation are some of the classical chemical synthesis routes. Precursor compounds have to be first calcined under air and second reduced by hydrogen or hydrides to receive MNPs. Physical synthesis routes include the application of microwaves, sonic waves, or supercritical fluids. Moreover, there are several protocols to deposit pre-prepared colloidal MNPs onto the surface of various supports [56]. This is a very interesting approach, because colloidal particles can be synthesized very uniformly with respect to size and shape [37, 56].

Supported metal catalysts are applied in large scale in several industries such as refining of petroleum, hydrogenation of carbon monoxide, hydrogenation of fats, and many other processes [43, 55, 56]. They are also the heart of automotive catalysts to clean automobile exhaust gases [57]. Such catalysts and the significance of a high dispersion are known for over hundred years, in particular, from various hydrogenation reactions. The hydrogenation of carbon monoxide to methane over supported nickel catalysts was discovered in the beginning of the last century by Sabatier and Senderens [58, 59]. This reaction is known today as “Sabatier reaction” or methanization, in general. It is applied in large scale in industry to remove traces of CO from ammonia synthesis gas, but it also gains importance in energy-storage efforts by converting solar energy via hydrogen to storable methane [60]. In this process chain, CO₂ reacts nearly quantitatively with hydrogen to methane over Ni or NiRu containing catalysts at about 300–350°C, with H₂:CO₂ feed ratio of 4 and slightly increased pressure up to 10 bar [60, 61]. Paul Sabatier received together with Victor Grignard the Noble Prize in Chemistry in 1912 for his method of hydrogenating organic compounds in the presence of finely disintegrated metals, whereby the progress of organic chemistry has been greatly advanced in recent years [62]. The explanatory statement explicitly points to the necessity of the “finely disintegrated metals” that we know today as metal nanoparticles.

One of the most common hydrogenation catalyst formulation is nickel on oxidic (e.g., alumina, zirconia, ceria, titania, or silica) [55, 63, 64] or carbon [65, 66] supports. As mentioned above, such catalysts are normally used as methanization catalysts, and other applications are also in common use such as catalysts, for example, for hardening of oils and fats in food industry, dry reforming of methane to manufacture syngas by using CO₂ [67, 68], or in petrochemical industries and refinery. In the latter case, they are of interest in the hydrogenation of various aromatic compounds to reduce their content in fuels. Nickel-containing catalysts are also in large-scale operation with respect to SRM reaction to generate hydrogen and/or syngas (CO, H₂) [53, 69]. The SRM reaction is carried out in general over Ni/alumina catalysts at around 800°C. Additional hydrogen can be manufactured by the water gas shift (WGS) reaction converting CO and water to CO₂ and H₂. The WGS reaction is industrially carried out using supported high-temperature shift FeCr (350–500°C) and low-temperature shift CuZn catalysts (180–250°C), respectively [70, 71]. Nowadays, this reaction gains much importance for ion fuel cell applications too [72]; mainly nonnoble metals such as Cu or Ni on ceria are under development [71].

Nickel-containing catalysts play an increasing role in chemical transformation of biomass-derived feedstock. Song et al. studied Ni on various carbons or MgO supports for depolymerization of lignosulfonate and identified three Ni functions being (i) the active sites for hydrogenolysis of C–O–C bonds; (ii) as active sites for hydrogenolysis of C–OH bonds at side chains to alkane chains, and (iii) as convertors for sulfonate to H₂S [73]. In a detailed study on hydrodeoxygenation of phenol as model compound and pyrolysis oil as a real feed, we recently could show the potential of bimetallic NiCo NPs supported on zeolite supports [74].

Further examples of the industrial application of SMNP catalysts are FT synthesis of hydrocarbons over Co, Fe, Ni, Ru catalysts [75, 76] or the synthesis of ethylene oxide from ethylene and oxygen over Ag/alumina [77, 78]. Another good example is the use of sulfided CoMo and

NiMo catalysts in refinery industry for the removal of sulfur from different distillation cuts by special hydrodesulfurization (HDS) units [79]. Mainly alumina is used as support; however, improvements in deeper HDS are reached by a variation of supports (silicas, zeolites, amorphous aluminosilicates, etc.) or the addition of further (noble) metals to the conventional catalyst composition [80, 81].

Besides these applications in well-studied industrial fields, novel SMNP materials are manufactured in recent years that might lead to new catalyst developments with respect to synthesis procedures, catalyst performance, and possible applications. Novel support materials like carbon nanotubes [82], graphene oxide [83], or carbon nitrides [84] might lead to novel interactions with MNPs resulting in novel catalysts. Jin et al. recently reported on the use of mesoporous metal oxide microspheres as support for Pd NPs and their use in reduction of nitro compounds [85]. Increasingly, noble metals are replaced by transition metals, or their alloys lead to cheaper catalysts, improved performance, NP stability, and/or new applications [37, 60, 86].

4. Green catalytic application of metal nanoparticles

Even though most of the catalysts are made by mixing and shaking some components, their surface structures are not yet well controlled. For any catalyst, it is desired to achieve long life cycle, 100% selectivity, and low energy consumptions, and these properties can only be gained by controlling their size, shape, electronic structure, and chemical and thermal stabilities of catalyst particles [87]. In the case of dealing with catalysts in the nanoscale level, selectivity ratio can be adjusted by precisely controlling the size of nanoparticles. Hence, precious metallic catalysts are usually used in the form of nanoparticles to improve their selectivity.

Nanocatalysts are used in chemical processing industries due to their lower energy consumption, environment-friendly behavior, with an improved economy. For instance, nanocatalysts of NiO with novel aluminum oxide support are used in the production of syngas and bio-oil from pyrolysis of biomass. Nanocatalysts improved the quality of syngas by decreasing the fraction of carbon monoxide in the syngas; it also reduced the proportion of tar in the product [88, 89].

Biomass energy is fulfilling about 15% of total energy requirement of the world; the broad range of organic materials included wood, crops, organic wastes (animal dung, municipal wastes, etc.), which are used for the production of biomass energy. And mostly, these materials are produced from the process of photosynthesis; according to the study of Luo and Demirbas, approximately 720 tons of biomass are produced per year [90, 91]. There are three main types of reactions for the conversion of biomass into fuel energy, such as combustion, pyrolysis, and gasification. Pyrolysis technique is preferred on other techniques due to its product named as pyrolytic oil or bio-oil. High moisture content, long-chain hydrocarbon, and low hydrogen-carbon ratio make it difficult to burn. Therefore, mainly biofuel is not directly used as fuel. Aravind [92] and Malik [93] studied the effect of nanocatalysts on the processing of bio-oil into syngas and concluded that nanoparticles with high surface area are the best alternatives of

conventional catalysts to improve the yield of syngas. Tar is an undesirable by-product in syngas production due to its high boiling point, and hence it blocks the filter and pipes. Tar is also a poison to the catalyst [94]. There are two methods to control the production of tar: one is treatment within gasifier and the second one is hot gases treatment after the gasifier. The second method is most economical, and hence it is only used in industries. Nanocatalysts of sodium, potassium, and calcium are used for hot gases treatment of effluent to reduce the amount of tar [95]. Catalytic reforming of tar by using metallic nanocatalysts is preferred because there is no need for any additional energy, and that is the reason why nanocatalysts are called green catalysts. This catalytic reaction also includes steam reforming, hydrocracking, and hydroreforming [96, 97].

In the Fischer-Tropsch synthesis of green diesel, nanocatalysts of iron and Co of size 10–15 nm are used in slurry reactors to improve the production of high molecular waxes. These waxes then hydrocracked to generate green diesel [98, 99]. Fischer-Tropsch's is an important method to convert nanopetroleum feedstock such as coal and biomass into clean diesel, which can be used as a fuel. Uses of nanocatalysts dramatically decrease the cost of this process as reported elsewhere [100].

FT syntheses technology produced high-quality ultraclean fuel with low aromatic content and zero sulfur. The product mostly consists of the mixture of linear and branched hydrocarbons [101]. Two types of techniques are adopted for FT synthesis, but the slurry bubble column techniques gain more interest due to its low pressure and stable temperature [102]. Generally, the Fischer-Tropsch synthesis follows the ASF distribution mechanism, but this distribution is unselective in this case. Later on, the novel Fischer-Tropsch catalysts are developed; the novel FT nanocatalyst containing Co with porous silica support is more selective toward hydrocarbons of C_{10} – C_{20} (diesel) [103]. Study of Kang et al. [99] showed that the nanocatalyst of Ru is more favorable in the high moisture content, but the only issue they have is low activity. This issue was solved by using carbon nanotube supported ruthenium catalyst, which gives excellent selectivity for diesel hydrocarbons and also high activity of the catalyst [99, 104].

Solid catalysts of Aluminum dodecatungstophosphate ($Al_{0.9}H_{0.3}PW_{12}O_{40}$) or nanotubes of $Zn_{1.2}H_{0.6}PW_{12}O_{40}$ are used for esterification of waste cooking oil to produce biodiesel; these catalysts improved yield from 42.6 to 96%. It is due to improved surface area of the nanocatalysts from the bulk conventional catalyst [99]. Animal and used cooking oil are alternative sources of diesel fuel to run the vehicles [105]. However, high water content and the high ratio of free fatty acid make them unfavorable for the production of diesel fuel. Sulfuric acid with a large quantity of methanol at high temperature and pressure reduces the quantity of free fatty acids. High pressure and high temperature increase the diesel fuel production cost [106]. According to the study of Li et al., ZnPW nanotubes can be used to reduce free fatty acid at lower temperature and pressure [107].

MNPs are also used in fossil fuel sector to improve the reaction; selective hydrogenation, paraffin hydrogenation, naphtha reforming, and hydrodesulfurization are some of the major units where nanocatalysts are used in oil refineries. Nanoparticles hexanethiol monolayer-protected palladium of size 1.5 nm are used to improve energy consumption of catalytic

combustion of JP-10 activation fuel. These nanoparticles decrease the ignition temperature to 240°C [108, 109].

Meurig et al. [110] studied the bimetallic nanocatalysts of size range 3–30 nm with nanoporous silica support in single-step hydrogenation and found that this catalyst greatly facilitates the separation of product from reactant, with easy recycling at low temperature and pressure conditions.

Hydrogen gas can be used in fuel cell to generate green energy; now, almost 95% of hydrogen is produced by using partial oxidation and steam reforming of hydrocarbons. Both oxidation and steam reforming produce carbon dioxide, which is a major constituent of global warming [111]. Catalytic reforming of green biofuel such as ethanol can be a green way for the production of hydrogen gas; ethanol is usually available with high water content; the water present in ethanol and other impurities deactivate the conventional catalysts. Nicolas et al. [112] worked on the designing of nanocatalysts for the production of hydrogen gas by using ethanol and concluded that nanocatalyst rhodium metal with alumina support gives the highest yield of hydrogen gas with a better protection from water. Rhodium catalyst produces cleavage between carbon and hydrogen, and this is the main reason of C–C bond rupture. Hydrogen in fuel cell gives 50–60% efficiency, while in diesel engine only 20–25% fuel is converted into useful energy [113, 114].

In brief, MNPs are used to increase the selectivity and activity of catalyst, which resulted in less energy consumption and high yield. In general, the majority of the chemical reactions obtain on the surface of the catalyst and hence with decreasing size of particles there is an increase in catalytic activity. Slower reactions are caused by continuously decreasing the size of the metal nanoparticle catalysts whereas increasing the size of the catalyst will decrease the rate of reaction. Nanocatalysts are energy-efficient; they reduce global warming by reducing the required energy for any catalytic process with less poisoning ratio. They also decrease the chemical wastes; all these factors resulted into an improved economy and safer environment.

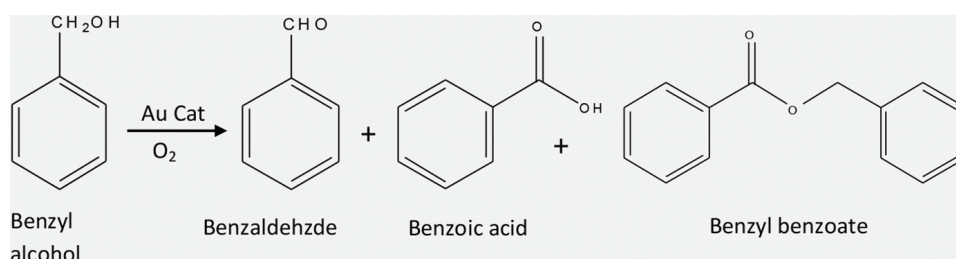
5. Own results

The nature of the support has great influence over MNPs' catalytic performance. This is because the support allows for efficient pathways to the target outcome, which compounds the impact of particle size stabilization when it comes to small MNPs' growth. Supports must have a strong metal-support interaction (SMSI), a high surface area, and incidence of active sites that can contribute to the reaction process [115]. This section investigates the catalytic application of MNPs, particularly for the oxidation of cyclohexane to adipic acid, the oxidation of benzyl alcohol to benzaldehyde, and the photodegradation of dyes. These reactions can be evaluated through the technique of placing MNPs on various kinds of metal oxide supports. The supports are used to afford high metal surface areas as well as stabilize the small MNPs characterized by high dispersion degrees [116]. Catalytic performance of heterogeneous reactions can also be affected by the support material characteristics, type of catalyst preparation method, degree of metal loading, and particle size. Specifically, supported noble metals

(e.g., gold) will have catalytic properties highly dependent on the type of support material at hand [116]. One example notes that acidic supports typically augment electron deficiencies on noble metals, when compared to basic supports. Strong metal-support interaction (SMSI) is demonstrated by metals supported on reducible oxides (e.g., TiO_2 and CeO_2) [117]. Robust interaction between the metallic components results in considerably higher catalytic activity compared to the catalysts having only one metal. This is in opposition to relatively inert irreducible oxides (e.g., Al_2O_3 , SiO_2). This section will examine five kinds of supports, taking into consideration the benefits derived from metal oxide supports. These different kinds have different impacts in terms of particle size, dispersion, and performance. The oxidation of benzyl alcohol and cyclohexane were both tested with these five supports described below, and the reactions were performed in the liquid phase. In addition, evaluation of gold nanoparticles supported on TiO_2 and ZnO will also be evaluated photocatalytically. The outcomes of these examinations are detailed below.

5.1. Oxidation of benzyl alcohol to benzaldehyde

Green chemistry emphasizes the importance of using oxidation to formulate chemical intermediates and fine chemicals with high selectivity [118], as is the case with forming benzaldehyde (BAI) from benzyl alcohol (BA) oxidation (**Scheme 1**). The resulting solution is frequently used in pharmaceutical, agrochemical, and perfume industries. Reaction of benzyl alcohol with excessive ammonium permanganate or potassium is possible in aqueous acidic medium to form benzaldehyde (BAI). However, this method has significant toxic by-products formation, and hence it is not really environment-friendly. Efforts have been made to amend this process by oxidizing benzyl alcohol using a green oxidant in the presence of organic solvent, such as H_2O_2 or O_2 , and applying various catalysts such as Pd/C, Pd(II) hydrotalcite, Pd-Ag/pumice, Ru-Co-Al hydrotalcite, Ni-containing hydrotalcite [119], but these techniques are still not considered to be environmentally acceptable due to the solvent use. Solvent-free oxidation is possible, using tert-Butyl hydroperoxide (TBHP) over MnO_4^{2-} -exchanged hydro-talcite and a transition metal containing layered double hydroxides and/or mixed hydroxides. However, this is not a clean process as the TBHP produces tert-butanol. To be considered clean and environmentally friendly, there must be no solvent used, and the oxidant ought to be molecular oxygen (i.e., clean and inexpensive). Prati et al. successfully demonstrated such a process using Au/C catalysts to selectively oxidize alcohols and polyols [120]. According to Rossi et al., gas-phase oxidation of volatile alcohols into aldehydes and ketones is possible using Au catalysts [121]. A similar process oxidizing glycerol to glyceric acid using Au/graphite catalysts was carried out by Carretin et al. [122], and was deemed to be fully selective of the target output. This high selectivity of Au/ CeO_2 was further proven by Abad et al. [123]. In case of benzyl alcohol oxidation to benzaldehyde, Enache et al. used supported Au on TiO_2 catalyst [124]. The same researchers also investigated the selective oxidation using Au-Pd alloy particles supported on TiO_2 [125]. In the end, the most efficient and environment-friendly means of oxidizing benzyl alcohol to benzaldehyde uses molecular oxygen. The technique also uses separable and recyclable supported gold nanoparticles over various metal oxide supports to provide high selectivity of the desired product, benzaldehyde.



Scheme 1. Oxidation of benzyl alcohol with O₂ using Au catalyst.

For the past several years, the oxidation of benzyl alcohol is being investigated specifically looking at the impact of different supported MNPs (such as Au nanoparticles) on various metal oxide carriers [120, 125]. In the present study, we have used different oxide supports (CaO, MgO, ZrO₂, Al₂O₃, TiO₂) for AuNPs that were prepared with impregnation techniques [126]. A range of spectroscopic and microscopic techniques was deployed to characterize these catalysts and gather data regarding their individual properties. Catalytic performance of the AuNPs was tested on solvent-free oxidation of benzyl alcohol with oxygen (5 bar) as an oxidant in a Parr autoclave reactor at a reaction temperature of 140°C. **Figure 5** demonstrates that Au catalyst performance is strongly dependent on the kind of applied support. Although BAI is the primary output, some by-products were also produced, including small amounts of benzyl benzoate, benzoic acid, and acetal. Benzyl benzoate occurs because of the additional esterification reactions due to benzoic acid and benzyl alcohol. Benzoic acid is a natural occurrence when benzaldehyde over-oxidizes. Finally, acetal is produced when benzyl alcohol does not react and instead forms hemiacetal, which eventually forms acetal through protonation and deprotonation reactions. Acetal occurred in this instance only to a smaller extent, which is however negligible in this case. The most active catalyst found is TiO₂-supported AuNPs (at

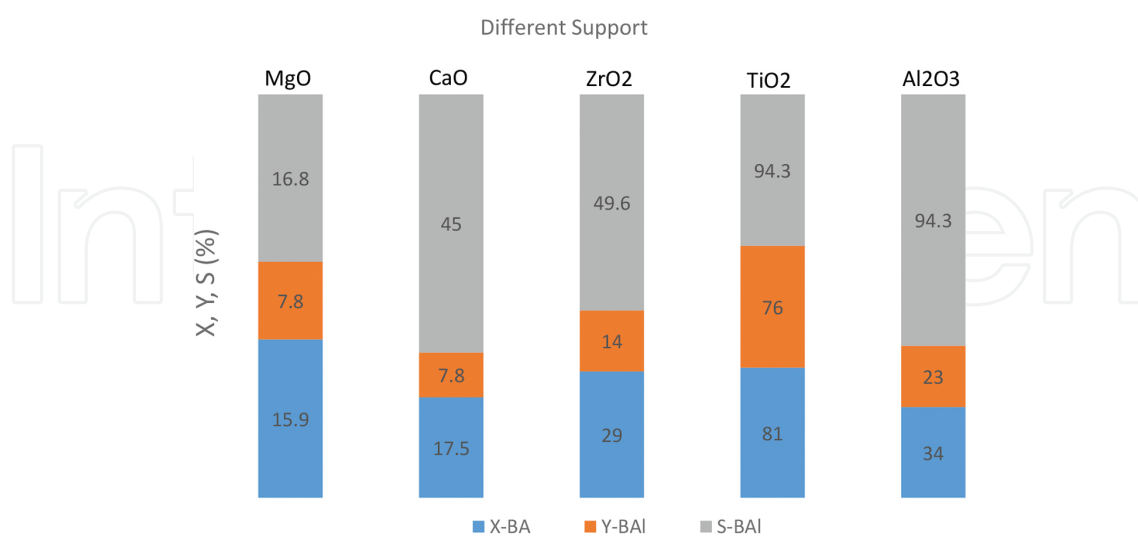
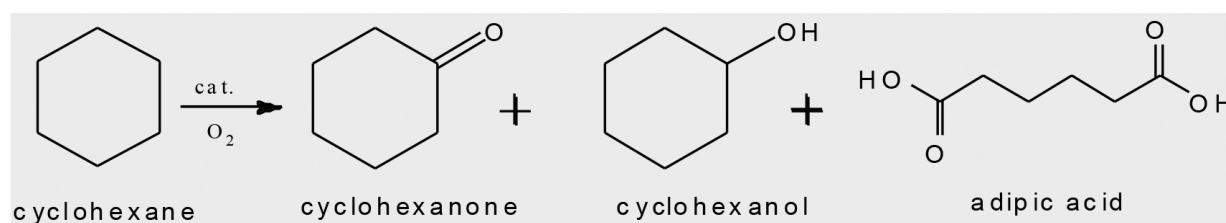


Figure 5. Influence of support on oxidation of benzyl alcohol to benzaldehyde over 1% Au/M catalysts ($M = \text{MgO}$, CaO , ZrO_2 , TiO_2 , Al_2O_3). Reaction conditions: 30 ml BA, 0.15 g catalyst, 140°C, 5 bar O₂, 4 h (X, conversion; Y, yield; S, selectivity).

X-BA = 81%), while the least active is MgO supported (at X-BA = 16% and S-BAI = 17%) (Figure 5). The enhanced performance of the former is due to several factors, including high dispersion of Au, smaller Au size, and comparatively greater surface enrichment of Au. These are completely opposite in the case of poor performing catalyst. TEM and XPS have been used to validate these claims.

5.2. Oxidation of cyclohexane to adipic acid

There are important industrial implications for selective oxidation of dicarboxylic acids from cycloaliphatic hydrocarbons, such as forming adipic acid (AA) from cyclohexane (CH) (Scheme 2). AA is a vital component when producing polyamides (such as nylon), polyesters, plasticizers (such as PVS), polyurethanes, and carpets. It is also used in the pharmaceutical and insecticides manufacturing processes [127], and has extensive applications for food products and medicines.

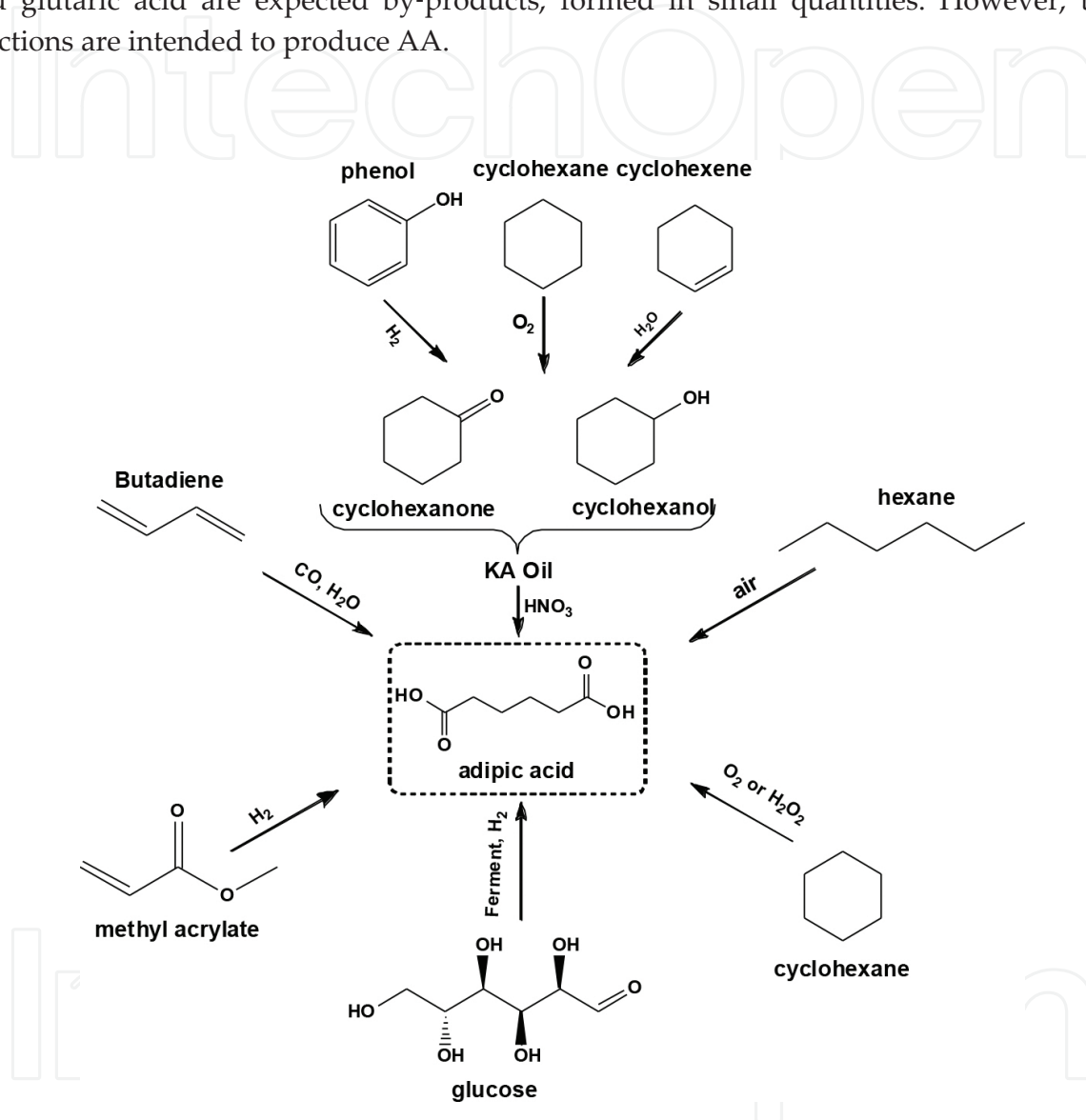


Scheme 2. Oxidation of cyclohexane with O₂ in the presence of nano-Au catalyst.

Commercial production of AA involves a two-stage process. Stage one requires oxidation of CH to create cyclohexanone (-One) and cyclohexanol (-Ol). This is done through the ketone and alcohol oil process (KA-oil) and operationalizes a cobalt or manganese catalyst at around 150°C and at 10-20 bar of air. Stage two derives AA from the KA-oil mixture by applying nitric acid as an oxidant [126]. The majority of AA is produced using this process. However, this process involves significant amount of recycling (more than 90%) of unreacted cyclohexane due to its low conversion (5–10%). The reaction is deliberately performed at such low conversion to obtain high selectivity (70–85%) of KA products. This recycling of ≥90% certainly incurs higher operation costs. Besides, there are also some additional environmental implications. Particularly, the usage of nitric acid in the second step results in the formation of NO_x by-products, which can be held responsible for smog, acid rain, and ozone depletion. Therefore, there is a need to explore new possible routes for the production of AA. This is the real motivation to uncover a more environment-friendly route using nano gold catalysts of the present study. **Scheme 3** depicts some other possible options for the production of AA. Although there are many potential options available, direct synthesis of AA from CH in a one-step process using O₂ is considered to be a more suitable option from both environment-friendly and economic points of view.

This research has also addressed oxidizing adipic acid from cyclohexane and the associated catalytic activity in addition to the oxidation of benzaldehyde from benzyl alcohol using supported AuNPs [126]. Section 5.1 outlines the type of catalysts used in this instance. The

reaction conditions applied for determining the influence of support in CH oxidation were: 10 ml CH, 20 ml solvent (acetonitrile), 0.3 g catalyst, 0.1 g TBHP, $pO_2 = 10$ bar, $t = 4$ h, 1500 rpm, $T = 130^\circ\text{C}$. The reaction resulted in adipic acid (AA), cyclohexanone (-One) and cyclohexanol (-Ol). Combining ketone and alcohol products is commonly denoted as KA (as is the case with commercially producing AA from cyclohexanone and cyclohexanol). Succinic acid, CO, CO_2 , and glutaric acid are expected by-products, formed in small quantities. However, these reactions are intended to produce AA.



Scheme 3. Summary of the different alternative pathways for AA production.

Figure 6 depicts the impact of the nature of oxide support on CH to AA oxidation activity. It is evident from the figure that the characteristics of the supports clearly influence both the product selectivity as well as CH conversion. It is also clear that AuNPs supported on TiO_2 gave the best performance compared to other supports. Similarly, even in case of benzyl alcohol oxidation, the same Au/ TiO_2 nanocatalyst was found to exhibit superior performance (**Figure 6**). The best performance of Au/ TiO_2 catalyst is due to (i) the formation of small AuNPs

(2–3 nm), (ii) high dispersion of Au, (iii) higher active metal (Au) area, and (iv) the high surface enrichment of Au species compared to other catalysts applied in this study [126]. This finding further confirms that catalyst performance is strongly dependent on the size of Au particles. As discussed earlier, the poor catalytic performance was observed over the MgO- and CaO-supported catalysts. In addition, these catalysts also produce high amounts of unwanted by-products (including CO and CO₂), and thus they should not be considered as appropriate supports for this reaction. Conversion of CH achieved over TiO₂ was 16.4%, and the selectivity of AA was 21.6%.

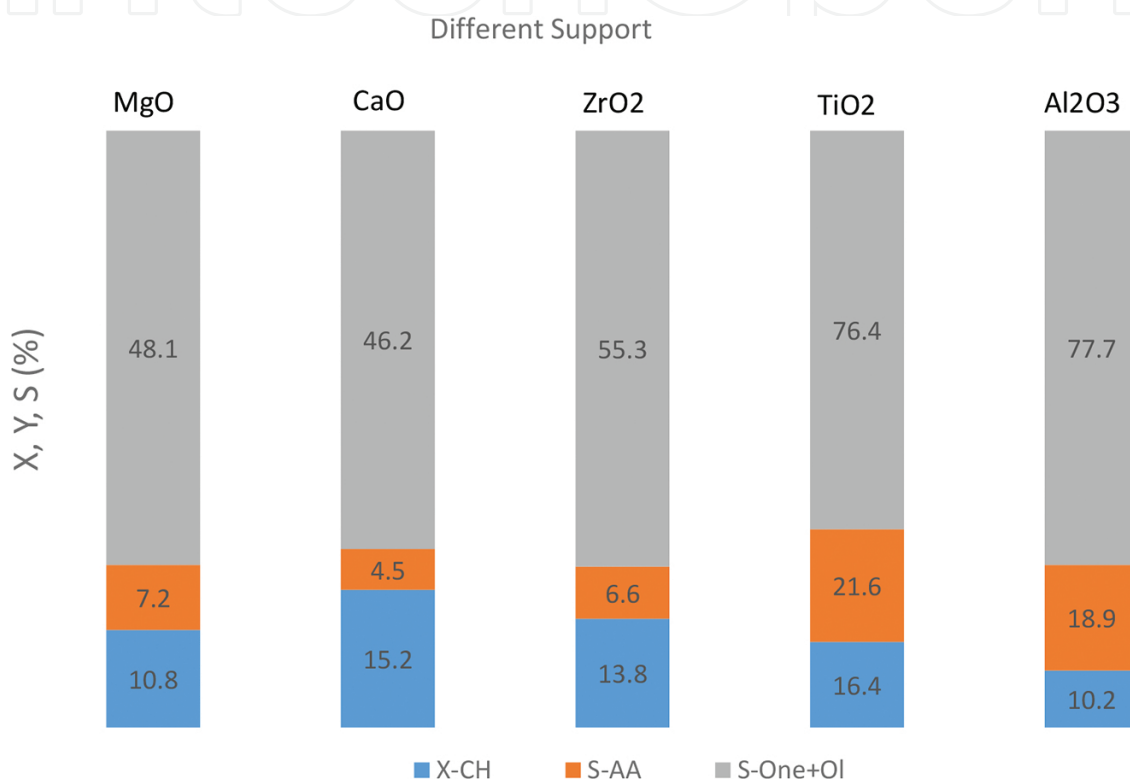


Figure 6. Effects of different oxide supports on the oxidation of cyclohexane over Au/X catalysts (X = MgO, CaO, ZrO₂, TiO₂, Al₂O₃). Reaction conditions: (10 ml CH, 20 ml solvent (acetonitrile), 0.3 g catalyst, 0.1 g TBHP, pO₂ = 10 bar, t = 4 h, 1500 rpm, T = 130°C). X-CH, conversion of cyclohexane; S-AA, selectivity of cyclohexane; S-One, selectivity of cyclohexanone; S-Ol, selectivity of cyclohexanol; S-Others, yields of glutaric acid, succinic acid, cyclohexylhydroperoxide, CO, and CO₂.

Moreover, we have also made attempts to find some correlations between the superior performances of AuNPs supported on TiO₂ compared to other types of catalysts. Such correlation between the Au particle size, surface gold-to-support atomic ratio (Au/SU) derived from XPS and catalytic performance is presented in **Figure 7**. It is clear from the figure that the activity results are in good agreement with the particle size of Au, and therefore the conversion of CH and selectivity to AA changed relatively in a similar way as that of Au size. Unsurprisingly, the smallest gold nanoparticles supported on TiO₂ showed the best catalytic activity. The conversion of CH decreased from 26% using Au/TiO₂ catalyst to 9% using Au/CaO. On the other hand, the Au size increased from 2 nm in case of using TiO₂ to 6–8 nm using CaO.

Moreover, the XPS results also confirmed that the surface region was indeed enriched in Au which hence the catalytic activity of gold catalyst. We can obviously observe from **Figure 7** that the gold nanoparticles supported on TiO_2 showed the highest surface Au/SU atomic ratios (SU = different supports) compared to others types of supports, and hence enhanced performance as well. In addition, supporting evidence for the beneficial effect of TiO_2 can be the high dispersion of Au and high active Au metal area. On the whole, better performance of TiO_2 is certainly due to the presence of small Au particles, high Au enrichment in the near-surface-region, high dispersion, and higher active metal area.

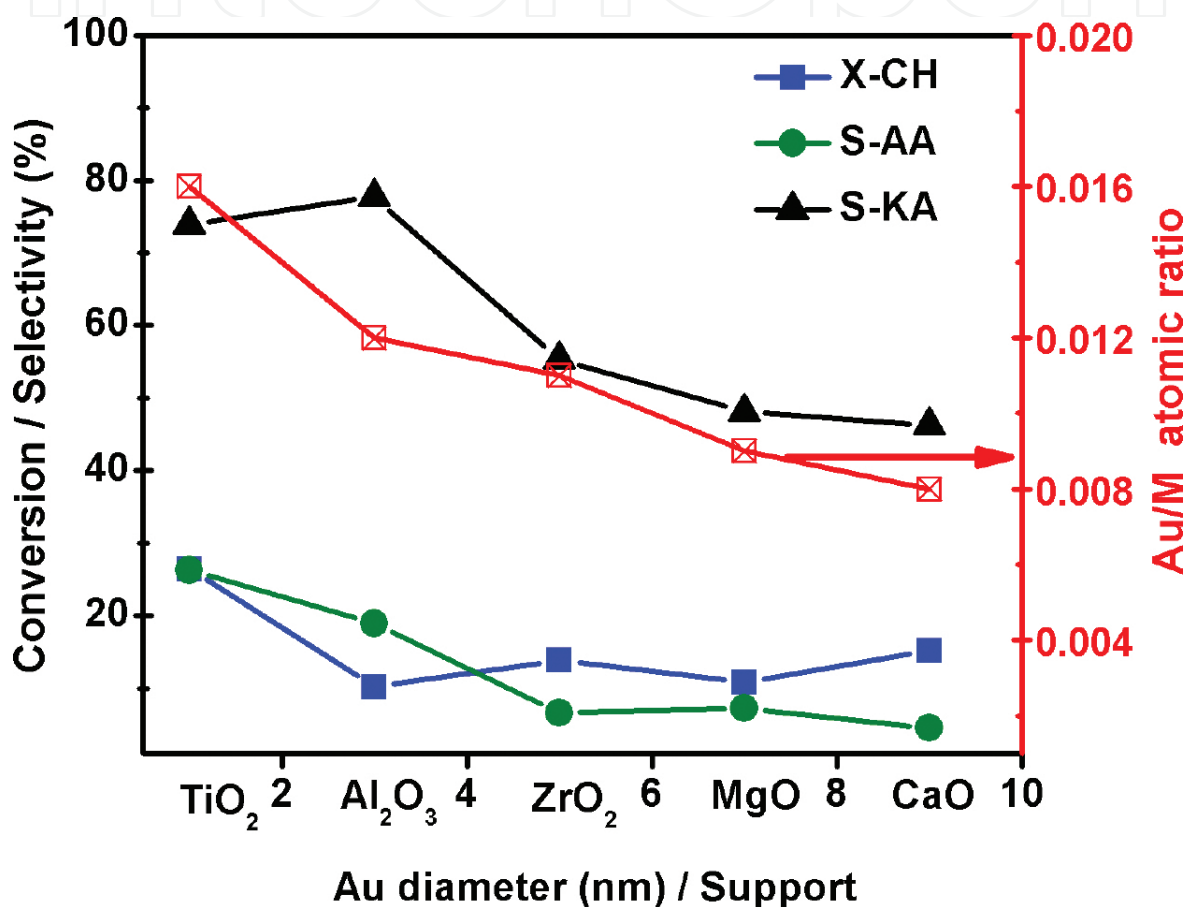


Figure 7. Correlation between cyclohexane conversion (X-CH), selectivity to adipic acid (S-AA) and to KA oil (S-KA), and catalyst properties of supported AuNPs.

5.3. Supported metal nanoparticles for dye's photodegradation

Metal nanoparticles (e.g., Au, Cu, and Ag) have recently begun to generate attention regarding their uses in electronics, optics, and the environment, and as catalysts [128–130]. One important green technology application is the use of combined M and metal oxide supports to remove dyes photocatalytically from water. Toward this end, we looked at the potential of using gold MNPs supported on TiO_2 and ZnO under UVA light irradiation to test their photocatalytic activity toward photodegradation of rhodamine B (RB) in aqueous medium [128]. The

procedure previously described was used to prepare the catalysts. The UV-vis absorption spectra of a 20 mg/L rhodamine B solution is demonstrated in **Figure 8a** and **b**, which shows the results before and after UVA light irradiation at 20-minute intervals and in the presence of one of two photocatalysts: Au/ZnO and Au/TiO₂. Even before introducing light irradiation, a test was deployed to determine if dye absorption transpired on the catalyst surface. According to the tests, there was a slight amount of absorption (as shown by a diminished RB concentration), which was comparable between the both photocatalysts applied. Peak absorption with Au/TiO₂ was observed to occur at 554 nm, and thereafter decreased during irradiation, until full elimination after 100 min (**Figure 8a**). Peak absorption with Au/ZnO occurred at RB 554 nm, and likewise decreased with exposure to irradiation, reaching full RB depletion at 80 min (**Figure 8b**). The former's 100-minute degradation time was slower, indicating that Au/ZnO has superior photocatalytic activity.

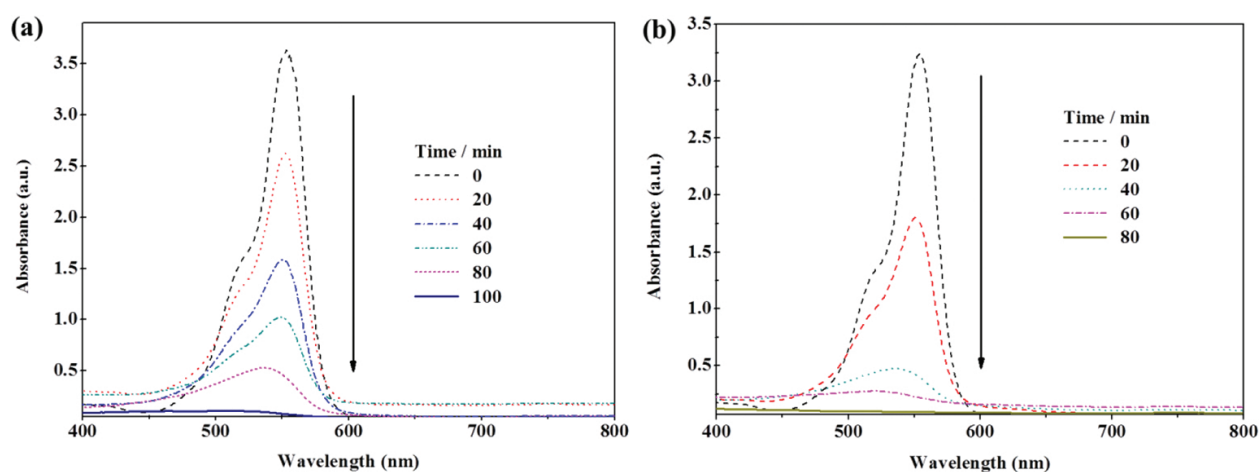


Figure 8. Absorption spectra of RB at different times after UV irradiation using Au/TiO₂ (a) and Au/ZnO (b) as AuNPs photocatalysts.

Furthermore, the degradation plot depicted in **Figure 9** shows further details, demonstrating the photocatalytic degradation of RB in aqueous medium using undoped and Au-doped photocatalysts, which is dependent on the nature of the support. For example, undoped TiO₂ and ZnO have similar RB photodegradation reactions in the first hour, with approximately 73% of the present RB dye present in the solution. Approximately 98% was achieved after 160 min, with constant efficiency following. It is possible that the photocatalytic performance was so stable beyond 160 min due to the accumulated degradation products at the photocatalyst surface. However, enhanced RB photodegradation performance was achieved by doping both TiO₂ and ZnO with 1 wt.% AuNPs. In this case, 87% degradation was achieved following 60 min with Au/TiO₂ and 96% with ZnO in the same time. Enhanced photocatalytic degrading capability could potentially be due to AuNPs' electron buffering, which results in slower recombination of pairs of electrons and holes [131]. Degradation efficiency of Au/ZnO rose to 97% when reaction time was increased to 80 min, and remained stable at this stage. Au/TiO₂ saw the same results when reaction time was increased to 100 min. This plateau behavior is likely due to reaction product deposits on the surface of the photocatalysts.

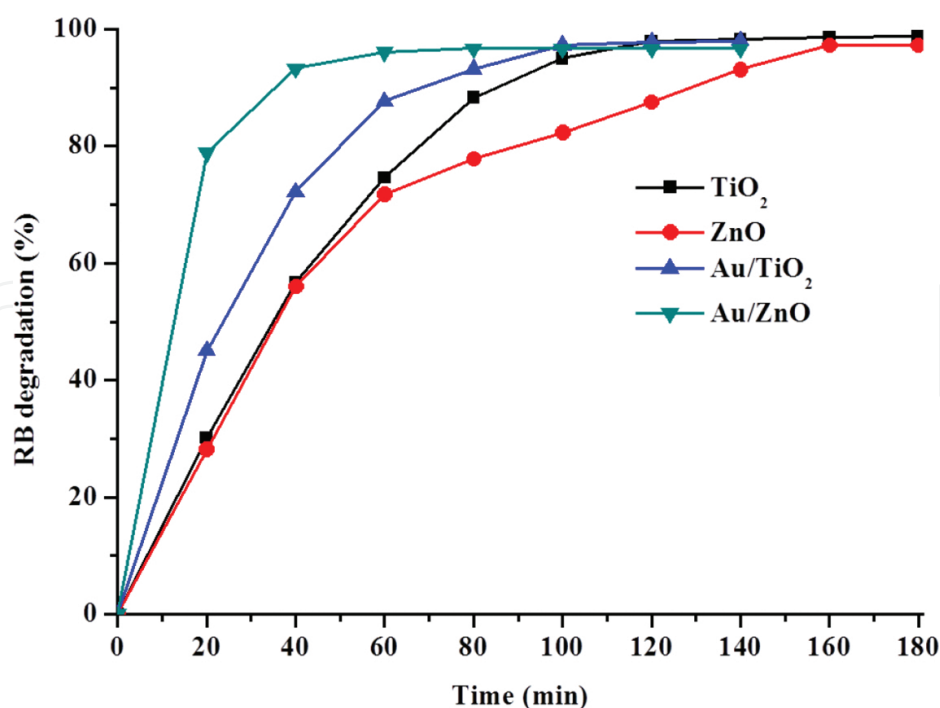


Figure 9. Photocatalytic degradation of RB under UV irradiation, catalyzed with TiO₂, ZnO, Au/TiO₂, and Au/ZnO.

6. Conclusions and outlook

Particles having the size from 1 to 100 nm are termed as nanoparticles, and in nanotechnology, small particles behave as an identical unit in both chemical and physical aspects. Supporting such metal nanoparticles is found to be a great tool where they can be used to develop different green catalytic applications. The interesting phenomenon about these materials is that their high surface area-to-volume ratio of solid-supported metal particles is essentially responsible for their catalytic properties. In this chapter, the recent reported methods for fabricating MNPs have been reviewed. However, the selection of such method is found to be dependent on the desired application. We have also shown that a deeper knowledge to understand the catalytic properties of MNPs is needed to explore the potential application of these MNPs. Therefore, different spectroscopic and microscopic techniques used to understand the catalytic parameters in MNPs have been briefly reviewed. A number of important green reactions using supported MNPs have been presented in this chapter. Quite recently, we have successfully reported that supported MNPs catalyst is an efficient catalyst for different applications such as the oxidation of cyclohexane to adipic acid. Here, one can clearly notice that the size of Au and the nature of support applied matter a lot. In this context, smaller Au particles revealed superior performance compared to their corresponding counterparts. Based on this, the Au/TiO₂ exhibited the best performance compared to other catalysts of the same series for both benzyl alcohol oxidation to benzaldehyde and cyclohexane oxidation to adipic acid. In addition, the application of supported MNPs as efficient photocatalysts was also reported.

Overall, recent advances have been made in governing metal particle morphology, size, and synthetic methodology. Prior art research demonstrates that synthetic approaches and adjustments to chemical and redox environments can result in control over the final form and morphology of nanoparticles. Using oxide carriers to synthesize stable MNPs has environment-friendly implications due to the fact that MNPs have unique properties compared to bulk or isolated atoms. When these MNPs interact successfully with the support, they may stabilize the surface and may generate Lewis sites that may catalyze certain catalytic reactions. However, the interaction degree depends upon the kind of support applied. Therefore, MNPs have varied and new environment-friendly applications. In view of this, highly unsaturated systems are considered superior as they provide larger number of active surface metal sites that may allow efficient interactions between the support and active phases. The ability to stabilize and control other MNPs (such as Pd, Rh, Pt, etc.) would be an excellent advancement, allowing concepts and reactions now possible with homogenous catalysis to be used in a heterogeneous context. However, the commercial application is limited by their activity and selectivity properties. Stability and durability of supported MNPs have implications for productivity. The research presented here was driven by determining the role of supported MNPs in various reactions taking place, either in liquid or gas phase, as well as their associated catalytic processes. Future research may address the creation of bifunctional or multifunctional MNPs, which may have implications for existing reactions or even new outputs. Furthermore, rational approaches need to be worked out in the coming years to sequence various functionalities in the direction of developing novel, attractive, and ecofriendly nanostructured metal nanoparticles for various catalytic applications.

Author details

Ahmad Alshammari^{1*}, V. Narayana Kalevaru^{2*} and Andreas Martin²

*Address all correspondence to: aalshammari@kacst.edu.sa

*Address all correspondence to: narayana.kalevaru@catalysis.de

1 Materials Science Research Institute (MSRI), King Abdulaziz City for Science and Technology (KACST), Riyadh, Saudi Arabia

2 Department of Heterogeneous Catalytic Processes, Leibniz Institute for Catalysis, Rostock, Germany

References

- [1] Fahlman BD. What is Materials Chemistry? New York: Springer; 2011. DOI: 10.1007/978-94-007-0693-4

- [2] Nouailhat A. *An Introduction to Nanoscience and Nanotechnology*. New York: Wiley; 2010. DOI: 10.1002/9780470610954
- [3] Astruc D. *Nanoparticles and Catalysis*. New York: Wiley, 2008. DOI: 10.1002/9783527621323
- [4] Somorjai G, Borodko Y. Research in nanosciences—great opportunity for catalysis science. *Catalysis Letters*. 2001;76(1-2):1–5. DOI: 10.1023/A:1016711323302
- [5] Pasquato L, Rancan F, Scrimin P, Mancin F, Frigeri C. N-methylimidazole-functionalized gold nanoparticles as catalysts for cleavage of a carboxylic acid ester. *Chemical Communications*. 2000;(22):2253–4. DOI: 10.1039/b005244m
- [6] Haruta M, Daté M. Advances in the catalysis of Au nanoparticles. *Applied Catalysis A: General*. 2001;222(1):427–37. DOI: 10.1016/S0926-860X(01)00847-X
- [7] Brayner R, Viau G, Bozon-Verduraz F. Liquid-phase hydrogenation of hexadienes on metallic colloidal nanoparticles immobilized on supports via coordination capture by bifunctional organic molecules. *Journal of Molecular Catalysis A: Chemical*. 2002;182:227–38. DOI: 10.1016/S1381-1169(01)00469-1
- [8] Toshima N, Shiraishi Y, Teranishi T. Effect of additional metal ions on catalyses of polymer-stabilized metal nanoclusters. *Journal of Molecular Catalysis A: Chemical*. 2001;177(1):139–47. DOI: 10.1016/S1381-1169(01)00314-4
- [9] Dai J, Bruening ML. Catalytic nanoparticles formed by reduction of metal ions in multilayered polyelectrolyte films. *Nano Letters*. 2002;2(5):497–501. DOI: 10.1021/nl025547l
- [10] Pileni M. Nanosized particles made in colloidal assemblies. *Langmuir*. 1997;13(13):3266–76. DOI: 10.1021/la960319q
- [11] Fu X, Wang Y, Wu N, Gui L, Tang Y. Shape-selective preparation and properties of oxalate-stabilized Pt colloid. *Langmuir*. 2002;18(12):4619–24. DOI: 10.1021/la020087x
- [12] Toshima N, Kuriyama M, Yamada Y, Hirai H. Colloidal platinum catalyst for light-induced hydrogen evolution from water. A particle size effect. *Chemistry Letters*. 1981;10(6):793–6. DOI: 10.1246/cl.1981.793
- [13] Hirai H, Chawanya H, Toshima N. Colloidal palladium protected with poly (N-vinyl-2-pyrrolidone) for selective hydrogenation of cyclopentadiene. *Reactive Polymers, Ion Exchangers, Sorbents*. 1985;3(2):127–41. DOI: 10.1016/0167-6989(85)90055-8
- [14] Yonezawa T, Toshima N. Mechanistic consideration of formation of polymer-protected nanoscopic bimetallic clusters. *Journal of the Chemical Society, Faraday Transactions*. 1995;91(22):4111–9. DOI: 10.1039/ft9959104111
- [15] Toshima N, Hirakawa K. Polymer-protected bimetallic nanocluster catalysts having core/shell structure for accelerated electron transfer in visible-light-induced hydrogen generation. *Polymer Journal*. 1999;31:1127–32. DOI: 10.1295/polymj.31.1127

- [16] Li Y, El-Sayed MA. The effect of stabilizers on the catalytic activity and stability of Pd colloidal nanoparticles in the Suzuki reactions in aqueous solution. *The Journal of Physical Chemistry B*. 2001;105(37):8938–43. DOI: 10.1021/jp010904m
- [17] Klingelhöfer S, Heitz W, Greiner A, Oestreich S, Förster S, Antonietti M. Preparation of palladium colloids in block copolymer micelles and their use for the catalysis of the Heck reaction. *Journal of the American Chemical Society*. 1997;119(42):10116–20. DOI: 10.1021/ja9714604
- [18] Kimling J, Maier M, Okenve B, Kotaidis V, Ballot H, Plech A. Turkevich method for gold nanoparticle synthesis revisited. *The Journal of Physical Chemistry B*. 2006;110(32):15700–7. DOI: 10.1021/jp061667w
- [19] Swihart MT. Vapor-phase synthesis of nanoparticles. *Current Opinion in Colloid & Interface Science*. 2003;8(1):127–33. DOI: 10.1016/S1359-0294(03)00007-4
- [20] Kruis FE, Fissan H, Peled A. Synthesis of nanoparticles in the gas phase for electronic, optical and magnetic applications—a review. *Journal of Aerosol Science*. 1998;29(5): 511–35. DOI: 10.1016/S0021-8502(97)10032-5
- [21] Okazaki K-i, Kiyama T, Hirahara K, Tanaka N, Kuwabata S, Torimoto T. Single-step synthesis of gold–silver alloy nanoparticles in ionic liquids by a sputter deposition technique. *Chem Commun*. 2008;(6):691–3. DOI: 10.1039/B714761A
- [22] Li S, El-Shall MS. Synthesis of nanoparticles by reactive laser vaporization: silicon nanocrystals in polymers and properties of gallium and tungsten oxides. *Applied Surface Science*. 1998;127:330–8. DOI: 10.1016/S0169-4332(97)00651-X
- [23] Ullmann M, Friedlander SK, Schmidt-Ott A. Nanoparticle formation by laser ablation. *Journal of Nanoparticle Research*. 2002;4(6):499–509. DOI: 10.1023/A:1022840924336
- [24] Kammler HK, Mädler L, Pratsinis SE. Flame synthesis of nanoparticles. *Chemical Engineering & Technology*. 2001;24(6):583–96. DOI: 10.1002/1521-4125(200106)24:6<583::AID-CEAT583>3.0.CO;2-H
- [25] Stark WJ, Pratsinis SE. Aerosol flame reactors for manufacture of nanoparticles. *Powder Technology*. 2002;126(2):103–8. DOI: 10.1016/S0032-5910(02)00077-3
- [26] Rao N, Girshick S, Heberlein J, McMurry P, Jones S, Hansen D, et al. Nanoparticle formation using a plasma expansion process. *Plasma Chemistry and Plasma Processing*. 1995;15(4):581–606. DOI: 10.1007/BF01447062
- [27] De La Veaux SC, Zhang L. Method of producing nanoparticles using an evaporation-condensation process with a reaction chamber plasma reactor system. Google Patents; 2010.
- [28] Kotov YA. Electric explosion of wires as a method for preparation of nanopowders. *Journal of Nanoparticle Research*. 2003;5(5-6):539–50. DOI: 10.1023/B:NANO.000006069.45073.0b

- [29] Mao Z, Zou X, Liu X, Wang X, Jiang W, editors. Study of nanopowder production by gas-embedded electrical explosion of wire. 17th International Conference on High Power Particle Beams (Beams'08) in Xi'an, Shaanxi, China.
- [30] Jaworek A. Micro-and nanoparticle production by electrospraying. *Powder Technology*. 2007;176(1):18–35. DOI: 10.1016/j.powtec.2007.01.035
- [31] Srivastava SK, Yamada R, Ogino C, Kondo A. Biogenic synthesis and characterization of gold nanoparticles by *Escherichia coli* K12 and its heterogeneous catalysis in degradation of 4-nitrophenol. *Nanoscale Research Letters*. 2013;8(1):1–9. DOI: 10.1186/1556-276X-8-70
- [32] Parida UK, Bindhani BK, Nayak P. Green synthesis and characterization of gold nanoparticles using onion (*Allium cepa*) extract. *World Journal of Nano Science and Engineering*. 2011;1(04):93. DOI: 10.4236/wjnse.2011.14015
- [33] Petla RK, Vivekanandhan S, Misra M, Mohanty AK, Satyanarayana N. Soybean (*Glycine max*) leaf extract based green synthesis of palladium nanoparticles. *Journal of Biomaterials and Nanobiotechnology*. 2012;3:14–19. DOI: 10.4236/jbnt.2012.31003.2011
- [34] Lee JH, Ahn K, Kim SM, Jeon KS, Lee JS, Yu IJ. Continuous 3-day exposure assessment of workplace manufacturing silver nanoparticles. *Journal of Nanoparticle Research*. 2012;14(9):1–10. DOI: 10.1007/s11051-012-1134-8
- [35] Yang H, Wang Y, Huang H, Gell L, Lehtovaara L, Malola S, et al. All-thiol-stabilized Ag₄₄ and Au₁₂Ag₃₂ nanoparticles with single-crystal structures. *Nature Communications*. 2013;4:2422. DOI: 10.1038/ncomms3422
- [36] Prieto G, Zečević J, Friedrich H, de Jong KP, de Jongh PE. Towards stable catalysts by controlling collective properties of supported metal nanoparticles. *Nature Materials*. 2013;12(1):34–9. DOI: 10.1038/nmat3471
- [37] An K, Somorjai GA. Size and shape control of metal nanoparticles for reaction selectivity in catalysis. *ChemCatChem*. 2012;4(10):1512–24. DOI: 10.1002/cctc.201200229
- [38] Bell AT. The impact of nanoscience on heterogeneous catalysis. *Science*. 2003;299(5613):1688–91. DOI: 10.1126/science.1083671
- [39] Cuenya BR. Synthesis and catalytic properties of metal nanoparticles: size, shape, support, composition, and oxidation state effects. *Thin Solid Films*. 2010;518(12):3127–50. DOI: 10.1016/j.tsf.2010.01.018
- [40] Haruta M, Daté M. Advances in the catalysis of Au nanoparticles. *Applied Catalysis A: General*. 2001;222(1):427–37. DOI: 10.1016/S0926-860X(01)00847-X
- [41] Haruta M. Gold as a novel catalyst in the 21st century: preparation, working mechanism and applications. *Gold Bulletin*. 2004;37(1-2):27–36. DOI: 10.1007/BF03215514
- [42] Boudart M. Catalysis by supported metals. In: Frankenburg WG. *Advances in Catalysis*. 20th ed. New York: Academic Press; 1969. p. 153–66. ISSN:0360-0564

- [43] Gates BC. Supported metal clusters: synthesis, structure, and catalysis. *Chemical Reviews*. 1995;95(3):511–22. DOI: 10.1021/cr00035a003
- [44] Flytzani-Stephanopoulos M, Gates BC. Atomically dispersed supported metal catalysts. *Annual Review of Chemical and Biomolecular Engineering*, 2012;3:545–74. DOI: 10.1146/annurev-chembioeng-062011-080939
- [45] Borodzinski A, Bonarowska M. Relation between crystallite size and dispersion on supported metal catalysts. *Langmuir*. 1997;13(21):5613–20. DOI: 10.1021/la962103u
- [46] Hammer B, Morikawa Y, Nørskov JK. CO chemisorption at metal surfaces and overlayers. *Physical Review Letters*. 1996;76(12):2141. DOI: 10.1103/PhysRevLett.76.2141
- [47] Dulaurent O, Bianchi D. Adsorption isobars for CO on a Pt/Al₂O₃ catalyst at high temperatures using FTIR spectroscopy: isosteric heat of adsorption and adsorption model. *Applied Catalysis A: General*. 2000;196(2):271–80. DOI: 10.1016/S0926-860X(99)00472-X
- [48] Joshi AM, Tucker MH, Delgass WN, Thomson KT. CO adsorption on pure and binary-alloy gold clusters: a quantum chemical study. *The Journal of Chemical Physics*. 2006;125(19):194707. DOI: 10.1063/1.2375094
- [49] Mustard DG, Bartholomew CH. Determination of metal crystallite size and morphology in supported nickel catalysts. *Journal of Catalysis*. 1982;67(1):186–206. DOI: 10.1016/0021-9517(81)90271-2
- [50] Cui C, Gan L, Li HH, Yu SH, Heggen M, Strasser P. Octahedral PtNi nanoparticle catalysts: exceptional oxygen reduction activity by tuning the alloy particle surface composition. *Nano Letters*. 2012;12(11):5885–9. DOI: 10.1021/nl3032795
- [51] Stamenkovic VR, Mun BS, Arenz M, Mayrhofer KJ, Lucas CA, Wang G, Ross PN, Markovic NM. Trends in electrocatalysis on extended and nanoscale Pt-bimetallic alloy surfaces. *Nature Materials*. 2007;6(3):241–7. DOI: 10.1038/nmat1840
- [52] Chin YHC, King DL, Roh HS, Wang Y, Heald SM. Structure and reactivity investigations on supported bimetallic Au Ni catalysts used for hydrocarbon steam reforming. *Journal of Catalysis*. 2006;244(2):153–62. DOI: 10.1016/j.jcat.2006.08.016
- [53] Matsumura Y, Nakamori T. Steam reforming of methane over nickel catalysts at low reaction temperature. *Applied Catalysis A: General*. 2004;258(1):107–14. DOI: 10.1016/j.apcata.2003.08.009
- [54] Hayek K, Kramer R, Paál Z. Metal-support boundary sites in catalysis. *Applied Catalysis A: General*. 1997;162(1):1–15. DOI: 10.1016/S0926-860X(97)00243-3
- [55] White RJ, Luque R, Budarin VL, Clark JH, Macquarrie DJ. Supported metal nanoparticles on porous materials. Methods and applications. *Chemical Society Reviews*. 2009;38(2):481–94. DOI: 10.1039/B802654H

- [56] Jia CJ, Schüth F. Colloidal metal nanoparticles as a component of designed catalyst. *Physical Chemistry Chemical Physics*, 2011;13(7):2457–87. DOI: 10.1039/C0CP02680H
- [57] Heck RM, Farrauto RJ. Automobile exhaust catalysts. *Applied Catalysis A: General*. 2001;221(1):443–57. DOI: 10.1016/S0926-860X(01)00818-3
- [58] Sabatier P, Senderens JB. New synthesis of methane. *Comptes Rendus Hebdomadaires des Seances de l'Academie des Sciences*. 1902;134:514–516.
- [59] Sabatier P, Senderens JB. Direct hydrogenation of the oxides of carbon in the presence of various finely-divided metals. *Comptes Rendus Hebdomadaires des Seances de l'Academie des Sciences*. 1902;134:689–91.
- [60] Lange F, Armbruster U, Martin A. Heterogeneously-catalyzed hydrogenation of carbon dioxide to methane over RuNi-bimetallic catalysts. *Energy Technology*. 2015;3:55–62. DOI: 10/1002./ente.201402113
- [61] Schoder M, Armbruster U, Martin A. Heterogen-katalysierte Hydrierung von CO₂ zu Methan unter erhöhten Drücken. *Chemie Ingenieur Technik*. 2013;85:344–52. DOI: 10.1002/cite.201200112
- [62] http://www.nobelprize.org/nobel_prizes/chemistry/laureates/1912/
- [63] Guo M, Lu G. The regulating effects of cobalt addition on the catalytic properties of silica-supported Ni–Co bimetallic catalysts for CO₂ methanation. *Reaction Kinetics, Mechanisms and Catalysis*. 2014;113(1):101–13. DOI 10.1007/s11144-014-0732-0
- [64] Jackson SD, Willis J, Kelly GJ, McLellan GD, Webb G, Mather S, Moyes RB, Simpson S, Wells PB, Whyman R. Supported nickel catalysts: preparation and characterisation of alumina-, molybdena-, and silica-supported nickel, and the identification of reactive oxygen on these catalysts by exchange with isotopically labelled carbon dioxide. *Physical Chemistry Chemical Physics*. 1999;1:2573–80. DOI: 10.1039/A809293A
- [65] Auer E, Freund A, Pietsch J, Tacke T. Carbons as supports for industrial precious metal catalysts. *Applied Catalysis A: General*. 1998;173(2):259–71. DOI: 10.1016/S0926-860X(98)00184-7
- [66] Van de Vyver S, Geboers J, Schutyser W, Dusselier M, Eloy P, Dornez E, Seo JW, Courtine CM, Gaigneaux EM, Jacobs PA, Sels BF. Tuning the acid/metal balance of carbon nanofiber-supported nickel catalysts for hydrolytic hydrogenation of cellulose. *ChemSusChem*. 2012;5(8):1549–58. DOI: 10.1002/cssc.201100782
- [67] Gadalla AM, Bower B. The role of catalyst support on the activity of nickel for reforming methane with CO₂. *Chemical Engineering Science*. 1988;43(11):3049–62. DOI: 10.1016/0009-2509(88)80058-7
- [68] Chen YG, Ren J. Conversion of methane and carbon dioxide into synthesis gas over alumina-supported nickel catalysts. Effect of Ni–Al₂O₃ interactions. *Catalysis Letters*. 1994;29(1-2):39–48. DOI: 10.1007/BF00814250

- [69] Sehested J. Four challenges for nickel steam-reforming catalysts. *Catalysis Today*. 2006;111(1):103–10. DOI: 10.1016/j.cattod.2005.10.002
- [70] Ruettinger W, Ilinich O, Farrauto RJ. A new generation of water gas shift catalysts for fuel cell applications. *Journal of Power Sources*. 2003;118(1):61–5. DOI: 10.1016/S0378-7753(03)00062-4
- [71] Li Y, Fu Q, Flytzani-Stephanopoulos M. Low-temperature water-gas shift reaction over Cu- and Ni-loaded cerium oxide catalysts. *Applied Catalysis B: Environmental*. 2002;27(3):179–91. DOI: 10.1016/S0926-3373(00)00147-8
- [72] Ratnasamy C, Wagner JP. Water gas shift catalysis. *Catalysis Reviews*. 2009;51(3):325–440. DOI: 10.1080/01614940903048661
- [73] Song Q, Wang F, Xu J. Hydrogenolysis of lignosulfonate into phenols over heterogeneous nickel catalysts. *Chemical Communications*. 2012;48(56):7019–21. DOI: 10.1039/c2cc31414b
- [74] Huynh TM, Armbruster U, Pohl M-M, Schneider M, Radnik J, Hoang D-L, Phan BMQ, Nguyen DA, Martin A. Hydrodeoxygenation of phenol as a model compound for bio-oil over non-noble bimetallic catalysts based on Ni. *ChemCatChem*. 2016;6:1940–51. DOI: 10.1002/cctc.201402011
- [75] Schulz, H. Short history and present trends of Fischer–Tropsch synthesis. *Applied Catalysis A: General*. 1999;186(1):3–12. DOI: 10.1016/S0926-860X(99)00160-X
- [76] Khodakov AY, Chu W, Fongarland P. Advances in the development of novel cobalt Fischer–Tropsch catalysts for synthesis of long-chain hydrocarbons and clean fuels. *Chemical Reviews*. 2007;107(5):1692–744. DOI: 10.1021/cr050972v
- [77] Kim YC, Park NC, Shin JS, Lee SR, Lee YJ, Moon DJ. Partial oxidation of ethylene to ethylene oxide over nanosized Ag/ α -Al₂O₃ catalysts. *Catalysis Today*. 2003;87(1):153–62. DOI: 10.1016/j.cattod.2003.09.012
- [78] Rojluechai S, Chavadej S, Schwank JW, Meeyoo V. Catalytic activity of ethylene oxidation over Au, Ag and Au–Ag catalysts: support effect. *Catalysis Communications*. 2007;8(1):57–64. DOI: 10.1016/j.catcom.2006.05.029
- [79] Mortensen PM, Grunwaldt JD, Jensen PA, Knudsen KG, Jensen AD. A review of catalytic upgrading of bio-oil to engine fuels. *Applied Catalysis A: General*. 2011;407(1):1–19. DOI: 10.1016/j.apcata.2011.08.046
- [80] Prins R, De Beer VHJ, Somorjai GA. Structure and function of the catalyst and the promoter in Co–Mo hydrodesulfurization catalysts. *Catalysis Reviews – Science and Engineering*. 1989;31(1-2):1–41. DOI: 10.1080/01614948909351347
- [81] Babich IV, Moulijn JA. Science and technology of novel processes for deep desulfurization of oil refinery streams: a review. *Fuel*. 2003;82(6):607–31. DOI: 10.1016/S0016-2361(02)00324-1

- [82] Wildgoose GG, Banks CE, Compton RG. Metal nanoparticles and related materials supported on carbon nanotubes: methods and applications. *Small*. 2006;2(2):182–93. DOI: 10.1002/smll.200500324
- [83] Lightcap IV, Kosel TH, Kamat PV. Anchoring semiconductor and metal nanoparticles on a two-dimensional catalyst mat. Storing and shuttling electrons with reduced graphene oxide. *Nano Letters*. 2010;10(2):577–83. DOI: 10.1021/nl9035109
- [84] Li XH, Antonietti M. Metal nanoparticles at mesoporous N-doped carbons and carbon nitrides: functional Mott–Schottky heterojunctions for catalysis. *Chemical Society Reviews*. 2013;42(16):6593–604. DOI: 10.1039/c3cs60067j
- [85] Jin Z, Xiao M, Bao Z, Wang P, Wang J. A general approach to mesoporous metal oxide microspheres loaded with noble metal nanoparticles. *Angewandte Chemie International Edition*. 2012;51(26):6406–10. DOI: 10.1002/anie.201106948
- [86] Alayoglu S, Beaumont SK, Zheng F, Pushkarev VV, Zheng HM, Iablokov V, Liu Z, Guo JH, Kruse N, Somorjai GA. CO₂ hydrogenation studies on Co and CoPt bimetallic nanoparticles under reaction conditions using TEM, XPS and NEXAFS. *Topics in Catalysis*. 2011;54(13-14):778–785. DOI: 10.1007/s11244-011-9695-9
- [87] Satterfield CN. *Heterogeneous Catalysis in Practice*. New York: McGraw-Hill Companies; 1980.
- [88] Akia M, Yazdani F, Motaee E, Han D, Arandiyani H. A review on conversion of biomass to biofuel by nanocatalysts. *Biofuel Research Journal*. 2014;1(1):16–25. DOI: 10.18331/BRJ2015.1.1.5
- [89] Digman B, Joo HS, Kim DS. Recent progress in gasification/pyrolysis technologies for biomass conversion to energy. *Environmental Progress & Sustainable Energy*. 2009;28(1):47–51. DOI: 10.1002/ep.10336
- [90] Luo Z, Zhou J. Thermal Conversion of Biomass. *Handbook of Climate Change Mitigation*. New York: Springer; 2012. p. 1001–42. DOI: 10.1007/978-1-4419-7991-9_27
- [91] Demirbas A. Biofuels sources, biofuel policy, biofuel economy and global biofuel projections. *Energy Conversion and Management*. 2008;49(8):2106–16. DOI: 10.1016/j.enconman.2008.02.020
- [92] Aravind P, de Jong W. Evaluation of high temperature gas cleaning options for biomass gasification product gas for solid oxide fuel cells. *Progress in Energy and Combustion Science*. 2012;38(6):737–64. DOI: 10.1016/j.pecs.2012.03.006
- [93] Malik P, Sangwan A. Nanotechnology: a tool for improving efficiency of bio-energy. *Journal of Engineering and Applied Sciences*. 2012;1:37–49.
- [94] Asadullah M. Barriers of commercial power generation using biomass gasification gas: a review. *Renewable and Sustainable Energy Reviews*. 2014;29:201–15. DOI: 10.1016/j.rser.2013.08.074

- [95] Nzihou A, Stanmore B, Sharrock P. A review of catalysts for the gasification of biomass char, with some reference to coal. *Energy*. 2013;58:305–17. DOI: 10.1016/j.energy.2013.05.057
- [96] Anis S, Zainal Z. Tar reduction in biomass producer gas via mechanical, catalytic and thermal methods: a review. *Renewable and Sustainable Energy Reviews*. 2011;15(5):2355–77. DOI: 10.1016/j.rser.2011.02.018
- [97] Han J, Kim H. The reduction and control technology of tar during biomass gasification/pyrolysis: an overview. *Renewable and Sustainable Energy Reviews*. 2008;12(2):397–416. DOI: 10.1016/j.rser.2006.07.015
- [98] Boerrigter H, Den Uil H, Calis H-P. Green diesel from biomass via Fischer-Tropsch synthesis: new insights in gas cleaning and process design. *Citeseer*; 2003. p. 371–83.
- [99] Kang J, Zhang S, Zhang Q, Wang Y. Ruthenium nanoparticles supported on carbon nanotubes as efficient catalysts for selective conversion of synthesis gas to diesel fuel. *Angewandte Chemie*. 2009;121(14):2603–6. DOI: 10.1002/ange.200805715
- [100] Hutchings G, Polshettiwar V, Asefa T. *Nanocatalysis: Synthesis and Applications*. New York: John Wiley & Sons; 2013.
- [101] Fischer F, Tropsch H. The preparation of synthetic oil mixtures (synthol) from carbon monoxide and hydrogen. *Brennstoff-Chem*. 1923;4:276–85.
- [102] Saxena S, Rosen M, Smith D, Ruether J. Mathematical modeling of Fischer-Tropsch slurry bubble column reactors. *Chemical Engineering Communications*. 1986;40(1-6):97–151. DOI: 10.1080/00986448608911693
- [103] Van Der Laan GP, Beenackers A. Kinetics and selectivity of the Fischer-Tropsch synthesis: a literature review. *Catalysis Reviews*. 1999;41(3-4):255–318. DOI: 10.1081/CR-100101170
- [104] Serp P, Corrias M, Kalck P. Carbon nanotubes and nanofibers in catalysis. *Applied Catalysis A: General*. 2003;253(2):337–58. DOI: 10.1016/S0926-860X(03)00549-0
- [105] Ranganathan SV, Narasimhan SL, Muthukumar K. An overview of enzymatic production of biodiesel. *Bioresource Technology*. 2008;99(10):3975–81. DOI: 10.1016/j.biortech.2007.04.060
- [106] Zheng S, Kates M, Dube M, McLean D. Acid-catalyzed production of biodiesel from waste frying oil. *Biomass and Bioenergy*. 2006;30(3):267–72. DOI: 10.1016/j.biombioe.2005.10.004
- [107] Li J, Wang X, Zhu W, Cao F. $Zn_{1.2}H_{0.6}PW_{12}O_{40}$ nanotubes with double acid sites as heterogeneous catalysts for the production of biodiesel from waste cooking oil. *ChemSusChem*. 2009;2(2):177–83. DOI: 10.1002/cssc.200800208
- [108] Li S, Varatharajan B, Williams F. Chemistry of JP-10 ignition. *AIAA Journal*. 2001;39(12):2351–6. DOI: 10.2514/3.15032

- [109] Wickham DT, Cook R, De Voss S, Engel JR, Nability J. Soluble nano-catalysts for high performance fuels. *Journal of Russian Laser Research*. 2006;27(6):552–61. DOI: 10.1007/s10946-006-0034-8
- [110] Li S, Varatharajan B, Williams F. Chemistry of JP-10 ignition. *AIAA Journal*. 2001;39(12):2351–6. DOI: 10.2514/3.15032
- [111] Rostrup-Nielsen T. Manufacture of hydrogen. *Catalysis Today*. 2005;106(1):293–6. DOI: 10.1016/j.cattod.2005.07.149
- [112] Bion N, Duprez D, Epron F. Design of nanocatalysts for green hydrogen production from bioethanol. *ChemSusChem*. 2012;5(1):76–84. DOI: 10.1002/cssc.201100400
- [113] Schlapbach L, Züttel A. Hydrogen-storage materials for mobile applications. *Nature*. 2001;414(6861):353–8. DOI: 10.1038/35104634
- [114] Schlapbach L, Züttel A. Hydrogen-storage materials for mobile applications. *Nature*. 2001;414(6861):353–8. DOI: 10.1038/35104634
- [115] Kasta P, Friedricha M, Girgsdies F, Kröhnerta J, Teschnera D, Lunkenbeina T, Behrens M, Schlögl R. Strong metal-support interaction and alloying in Pd/ZnO catalysts for CO oxidation. *Catalysis Today*. 2016;260:21–30. DOI:10.1016/j.cattod.2015.05.021
- [116] Grisel RJH, Nieuwenhuys BE. Selective oxidation of CO, over supported Au. *Journal of Catalysis*. 2001;199(1):48–58. DOI:10.1006/jcat.2000.3121
- [117] Tauster SJ, Fung SC, Baker RTK, Horsley JA. Strong interactions in supported-metal catalysts. *Science*. 1981;211(4487):1121–5. DOI: 10.1126/science.211.4487.1121
- [118] Mallat T, Baiker A. Oxidation of alcohols with molecular oxygen on solid catalysts. *Chemical Reviews*. 2004;104(6):3037–58. DOI: 10.1021/cr0200116
- [119] Hashmi AS, GJ Hutchings. Gold catalysis. *Angewandte Chemie International Edition* 2006;45(47):7896–936. DOI: 10.1002/anie.200602454
- [120] Prati L, Rossi M. Gold on carbon as a new catalyst for selective liquid phase oxidation of diols. *Journal of Catalysis*. 1998;176(2):552–60. DOI:10.1006/jcat.1998.2078
- [121] Pina CD, Falletta E, Prati L, Rossi M. Selective oxidation using gold. *Chemical Society Reviews*. 2008;37:2077–95. DOI: 10.1039/B707319B
- [122] Carretin S, McMorn P, Johnston P, Griffin K, Kiely JC, Hutchings GJ. Oxidation of glycerol using supported Pt, Pd and Au catalysts. *Physical Chemistry Chemical Physics*. 2003;5:1329–36. DOI: 10.1039/B212047J
- [123] Abad A, Concepción P, Corma A, Garcíá HH. A collaborative effect between gold and a support induces the selective oxidation of alcohols. *Angewandte Chemie*. 2005;26(117):4134–7. DOI: 10.1002/ange.200500382.
- [124] Enache DI, Edwards JK, Landon P, Solsona-Espriu B, Carley AF, Herzing AA, Watanabe M, Kiely CJ, Knight DW, Hutchings GJ. Solvent-free oxidation of primary alcohols

to aldehydes using Au-Pd/TiO₂ catalysts. *Science*. 2006;311(5759):362–5. DOI: 10.1126/science.1120560

- [125] Miedziak P, Sankar M, Dimitratos N, Lopez-Sanchez JA, Carley AF, Knight DW, Taylor ST, Kiely CJ, Hutchings GJ. Oxidation of benzyl alcohol using supported gold–palladium nanoparticles. *Catalysis Today*. 2011;163(1):47–54. DOI:10.1016/j.cattod.2010.02.051
- [126] Alshammari A, Koeckritz A, Kalevaru VN, Bagabas A, Martin A. Significant formation of adipic acid by direct oxidation of cyclohexane using supported nano-gold catalysts. *ChemCatChem*. 2012;4(9):1330–6. DOI: 10.1002/cctc.201200008
- [127] Schuchardt U, Cardoso D, Sercheli R, Pereira R, Cruz RS, Guerreiro MC, Mandelli D, Spinace EV, Pires EL. Cyclohexane oxidation continues to be a challenge. *Applied Catalysis A: General*. 2001;211(1):1–17. DOI:10.1016/S0926-860X(01)00472-0
- [128] Alshammari A, Bagabas A, Assulami M. Photodegradation of rhodamine B over semiconductor supported gold nanoparticles: the effect of semiconductor support identity. *Arabian Journal of Chemistry*. 2014, in press.
- [129] Bagabas A, Alshammari A, Aboud M, Kosslick H. Room-temperature synthesis of zinc oxide nanoparticles in different media and their application in cyanide photodegradation. *Nanoscale Research Letters*. 2013;8(516):1–10. DOI: 10.1186/1556-276X-8-516
- [130] Alshammari A, Chi L, Chen X, Bagabas A, Kramer D, Alromaeha A, Zheng J. Visible-light photocatalysis on C-doped ZnO derived from polymer-assisted pyrolysis. *RSC Advances*. 2015;5:27690–8. DOI:10.1039/C4RA17227B
- [131] Yu H, Ming H, Gong J, Li H, Huang H, Pan K, Liu Y, Kang Z, Wei J, Wang, D. Facile synthesis of Au/ZnO nanoparticles and their enhanced photocatalytic activity for hydroxylation of benzene. *Bulletin of Materials Science*. 2013;36(3):367–72. DOI: 10.1007/s12034-013-0491-y

IntechOpen

